Delft University of Technology

Utilizing Process-Based Models to Better Incorporate Heterogeneities within Reservoir Modelling

Matthew Vacek

(4626052)

To obtain the degree of Master of Science
in Petroleum Engineering and Geosciences
at Delft University of Technology

To be defended publicly on October 2nd, 2018 at 1:30 pm

Thesis Committee:	Prof. Dr. A.W. Martinius	TU Delft, Equinor
	Dr. J.E.A. Storms	TU Delft
	Prof. Dr. R.W. Rossen	TU Delft
	Dr. H. Van der Vegt	TU Delft, Deltares

TU Delft Delft University of Technology

equinor

An electronic version of this thesis can be found at http://repository.tudelft.nl/.

Acknowledgements

Firstly, I would like to thank my thesis adviser, Allard Martinius. Without your guidance and extensive knowledge on the subject, the project would not have achieved the same results. The topic you provided helped me grow in different aspects of being a geologist. You constantly made sure that I had everything I needed to succeed and were always willing to answer any questions that I had. It was a great opportunity to work with a leader of industry and you have been a great inspiration to me.

I would also like to thank Helena van der Vegt. Your day-to-day guidance ensured that I was always on the correct path. You were always happy to answer my many questions, even those late on Sunday evenings. Our weekly discussions always ensured that I was on track and you were always there to help resolve an issues that I came across. You were very critical in the success of this project, and for that, I am extremely grateful.

Special thanks to the additional committee members, Joep Storms and Bill Rossen. You were always willing to take time to have a discussion even when I turned up unannounced. Your comments and suggestions helped guide the project to where it is now.

This thesis was funded by Equinor, and I am extremely grateful for their contribution and the trust they put in me. Their contribution allowed me to achieve the goals that we initially set forth at the beginning of the project. Once again, I would like to thank Allard for securing the funding for the project.

Lastly, I would like to thank my parents and my brother. Without their constant support and motivation throughout the duration of my studies, I would never have achieved what I have. You always believed in me no matter what. I am extremely grateful for everything you have provided for me over the years. Thank you.

Abstract

Traditional reservoir modelling utilizes a stochastic approach centered around statistics to generate a 3D representation of the reservoir. While the results of a stochastic approach are favorable, they tend to lack the detail that is necessary to fully understand the different aspects of the reservoir, more precisely, the inclusion of heterogeneities. A possible solution to this problem is the use of process-based models. Process-based models utilize the physical processes involved in the transportation, deposition, and erosion of sediments. As a result, the models generated are more complex in nature and better represent what is found within the subsurface. The use of process-based models within reservoir modelling is a a relatively new process that has yet to be fully utilized due to the difficulty in calibrating the models with well data. Before process-based models can be tested on their viability to include the multi-scalar heterogeneities, the model must be calibrated to match the real-world data. To test this, a combination of field work, lab work, and computer simulations is required. In this experiment, the Roda Sandstone Member, a Gilbert-type delta deposit in Northern Spain, was chosen as the unit of focus. The Roda Sandstone consists of multiple prograding sand lobes, with Roda Y being chosen as the focus of this experiment. The Roda Y sandstone exhibits a predominately medium and coarse grain distribution in the central locations of the sand lobe, and a fine and very fine distribution in the distal locations. Five simulations were run within the process-based modelling software "Delft3D", each with varying sediment input parameters, to observe the effects on the results. The results for the simulations show a strong calibration for each of the five simulations for coarse and medium grained sand, with a percent difference between the model results and the field data of 4-8%. The fine and very fine data contain a higher average difference between the two data sets, ranging from 18-23%. The difference for mud averages around 11%, with predominately more mud being deposited within the simulations. The large differences for the fine and very fine grained can be attributed to the difference in the size and shape of the sand lobe produced by the simulations. In locations were the two data points are equivalent in regards to depositional location within the sand lobe, a high correlation is observed. The results indicate that process-based models have the potential to be a very useful took within reservoir modelling. As this is the first step in a series of steps, additional testing is required for the additional aspects involved in utilizing process-based models to better incorporate heterogeneities within reservoir models.

Contents

List of Figures

List of Tables

1 Introduction:

The current determination and analysis of hydrocarbon volumes within a reservoir requires an understanding of various aspects of the reservoir; including sedimentological properties, reservoir architecture, and continuity of the sediments. Acquisition of reservoir data is typically achieved through direct measurements at the reservoir through a series of test wells. With the well data acquired, a stochastic model of the reservoir between the wells is generated. A 3D representation is then statistically interpolated between the wells and 3D reservoir is created. While stochastic and deterministic models have their advantages, they contain flaws as well. Stochastic models contain a series of complex events that use a relatively simple number of input parameters. The models that are generated are usually very basic in nature and do not properly represent what is actually present within the reservoir (Faculty and Institute of Actuaries, 1997). Using a statistical analysis provides insight on a large scale basis, but lacks many of the smaller geological details that are important when dealing with reservoir properties. The downsides associated with these models must be respected, otherwise the end product can vary drastically from what is actually found within the subsurface. When working with reservoir characterization, there are two main obstacles that must be overcome at the field appraisal stage when a limited amount of data is available: modeling of the sediment bodies to represent what is found in the subsurface, and secondly, to incorporate heterogeneities and specific sand bodies into the model in a way that reflects what is found within the depositional environment of the reservoir (Joseph, et al., 1993).

As mentioned above, one of the more complex issues involved in reservoir modeling is the inclusion of heterogeneities within the model. No two reservoirs are identical and each one must be individually analyzed to fully understand the characteristics of the reservoir. Understanding and incorporating the heterogeneities that are present, as well as their corresponding properties, is critical for properly analyzing the production capabilities of a reservoir.

This brings up the important question, what is the best way to incorporate these multi-scale heterogeneities within a reservoir model? Current models utilize a stochastic approach with a combination of statistics and object-based modelling. The results tend to lack complexity and contain high amounts of uncertainty. A possible solution to this problem is the incorporation of process-based modelling. Sedimentary process-based models incorporate the physical processes involved in the deposition and erosion of sediment (Koltermann & Gorelick, 1996; Karssenberg, Törnqvist, & Bridge, 2000). The main benefit of incorporating process-based models is that the results are more realistic in nature than models generated through stochastic methods. Process-based models have not been fully utilized in the oil and gas industry due to difficulties in conditioning the models to well and outcrop data (Clemetsen, Hurst, Knarud, & Omre, 1990). Process-based modelling allows the modeler to set the sensitivity of the model to include heterogeneities on a variety of scales. The smaller the heterogeneity, the smaller the grid scale, but at a cost of computational time. A modeling hypothesis must be set to correctly model the objective in the most accurate and efficient way possible. This thesis aims to show that process-based models can utilized to produce results that depict what is observed from outcrop data.

One of the issues involved with process-based modelling is that conditioning the model to represent subsurface data is typically very difficult. One way to overcome this obstacle is to utilize the reservoir architecture generated by process-based models as a 3D image to use in coordination with Multi-Point Statistical modelling. The combination of these two techniques has helped overcome the challenge of conditioning process-based models to the subsurface data. The lack of accurate training images still remains one of the main obstacles when dealing with multi-point statistical modelling (Mullins, Howell, van der Vegt, Buckley, & Storms, 2017).

The focus of this thesis is the calibration of a process-based model to represent data gathered from an outcrop. Before heterogeneities that are present within the reservoir can be incorporated into the process-based model, the model must be calibrated to represent the real-world data. If a model is not properly calibrated, the heterogeneities produced will not accurately depict the heterogeneities found within the reservoir. This will be one of the first times that process-based models will be used to replicate previously deposited sediments.

The process-based modelling software that was used in the simulations is Deltares' open-sourced program, Delft3D (Version 4.00.01). Delft3D is a modelling suite that incorporates sediment transport, morphology and hydrodynamics within fluvial and coastal environments. The program is extensively used to understand present day sediment transport and deposition within a fixed environment. This experiment is unique in that Delft3D was used to replicate a sand body that was deposited in the past; an unproven use of the program. If found to be successful, it could open a wide range of possibilities in the use of process-based models within the oil and gas industry. In the future, oil and gas companies could opt to utilize a process-based modelling technique for reservoir modelling in combination with a traditional stochastically generated model. This technique is especially promising for the exploration of hydrocarbons in the North Sea, due to the high abundance of oil and gas fields contained within ancient grabens. These grabens are similar in geological structure to that of the Tremp-Graus basin, which is the geological area of focus for this study.

The geological unit that was used to test this hypothesis is the Lower Eocene Roda Sandstone Member, located in the South-Central Pyrenean foreland basin. The Roda Sandstone is a group of terrigenous sands deposited in a Gilbert-type delta environment, bounded by fine-grained carbonate deposits. The Roda Sandstone is an example of a syntectonic deltaic deposit, which results in sediments being deposited during times of extensive rifting. The sandstone outcrops and is well exposed with very good lateral continuity throughout the study area, which results in the ability to perform various advanced sedimentological simulations (Tinterri, 2007). In the case of the Roda Sandstone, heterogeneities can range from thin mud laminations to tidal bundles that are meters in length and height. As a result, this presents a wide variety of opportunities to sample lateral variations within a single parasequence to better understand heterogeneity distribution and grain size distribution within an intra-parasequence scale before these small scale heterogeneities can be modelled, one must know the large scale sediment distribution and architecture of the sand lobe being studied.

2 Approach:

The aim of the project was to calibrate a process-based model of the Roda Sandstone to match the real-world data as closely as possible. The methodology to achieve this goal involved utilizing a combination of computer simulations, field work, and lab work. The approach involved a literature review of the Roda Formation and why this formation was chosen for the project. This provided background knowledge of the area and the formation. Field work in the Pyrenees Mountains in northern Spain was required to collect data from the field, as data from literature lacks the necessary detailed grain size distribution information. Field data is necessary as it acts as input parameters for the simulations, as well as to gauge the calibration of the final results. Field samples were collected from a variety of locations within the Roda Sandstone. After the field data was collected, a sample analysis, focused on grain size distribution, was performed to obtain the approximate input parameters, which were utilized within the simulations. Process-based models differ from stochastic models in the way that they are initially set up. Stochastic models are conditioned to well data and a 3D representation is generated for the space in between the wells. It is very difficult to condition process-based models to well or outcrop data, and therefore these models are only given initial conditions, allowing physics and the natural processes involved to control the model. Once the simulations were complete, the results were then compared to the outcrop data to test how well the model results matched to the real-world data. The model with the closest match was chosen and was further analyzed to determine locations of high and low differences within the model. Recommendations are made for future simulations that can improve the calibration of the models.

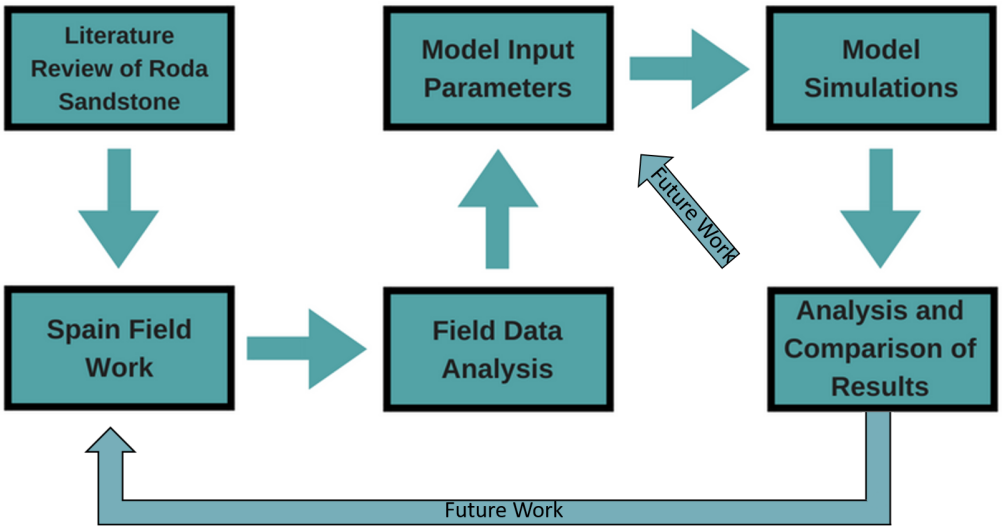

Figure 1: Workflow of the project and the steps involved to achieve the final results.

3 Geological Background

3.1 Regional Geology

The Roda Sandstone, part of the overall Roda Formation, is a siliciclastic unit in which the architectural elements are bounded by carbonate layers. The formation is located in the South-Central Pyrenean Foreland Basin, Northern Spain. The Pyrenees Mountains are described as a double-vergent orogenic belt which was created during the late Cretaceous to early Miocene as a result of the collision between the European and Iberian plates (Puigdefàbregas, Muñoz, & Vergés, 1992). The southern section of the Pyrenees can be characterized by south-vergent folding and thrusts represented by the axial zone basement and south Pyrenean cover thrusts sheets. As a result, the increased loading and flexing within the lithosphere gave rise to the east-west orientated South Pyrenean Foreland Basin (Tinterri, 2007).

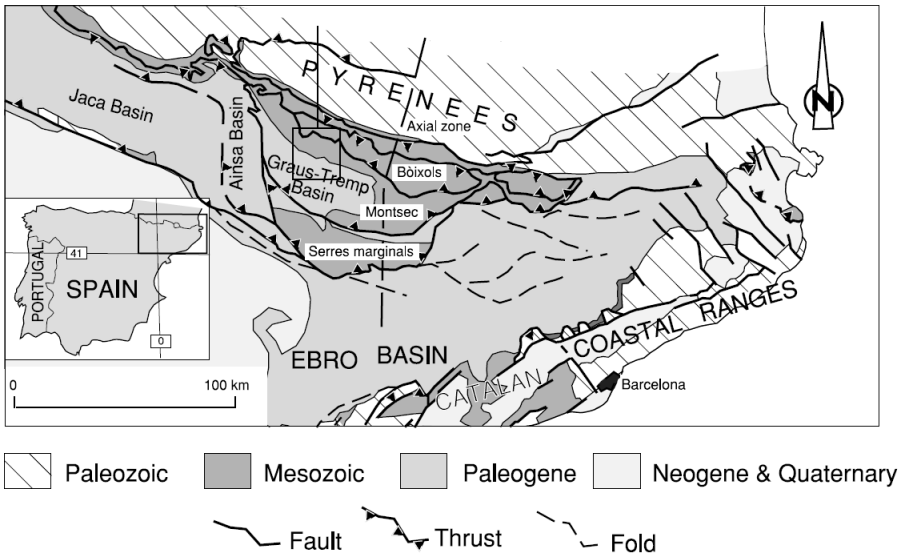

Figure 2: Regional Geology of North-East Spain (Lopez-Blanco 2003)

The Roda Formation is located within the Tremp-Graus Basin, a piggy back basin which was created between the Monstec and Boixols thrust sheets during the Paleocene-Early Eocene. The axial zone behind the sloping basin margin acts as the origin source for the sediments found within the basin (Michaud, 2011). The South Pyrenean Foreland Basin exhibits an east-west trend and contains an opening to the Atlantic Ocean on the western edge of the basin. Due to the effects of the southward moving thrust sheets, the South Pyrenean Foreland Basin exhibited substantial sea floor topography changes and over time was broken-up in a number of sub-basins, of which the Tremp-Graus Basin was formed. The basin is bounded in the west by an anticlinal topographic high which was formed due to the clockwise rotation of the east-west oriented Montsec thrust. Water depth in the basin during Roda times was variable and shallow (15 meters) in the east but deepening towards the west. Due to the shape of the basin, tides entered the basin from the west and proceed to the edge of the basin in the east. Once at the edge of the basin, the tides reverse direction and head west along the edge of the basin (Martinius, 2012).

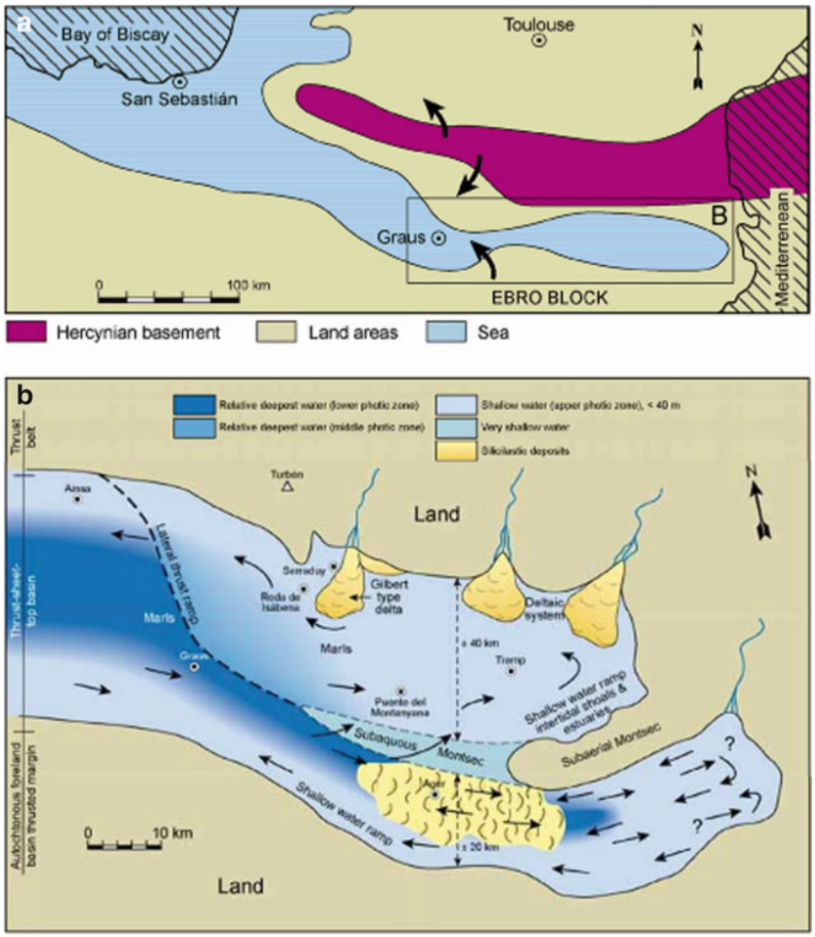

Figure 3: (A) Overview of the entire South Pyrenean Foreland Basin Complex. Hercynian basement is highlighted as it is believed to be the source of the Roda Sandstone. (B) Detailed section showing the Tremp-Graus basin and the adjacent Ager basin. Tidal movements are displayed as arrows originating from the west. (Martinius, 2012)

3.2 Sedimentological and Stratigraphic Background

The Roda Formation consists of two separate members: the younger Esdolomada Member and the Lower Eocene Roda Sandstone Member at the base. The interpretation of the Roda Sandstone Member has evolved throughout the years as more studies have been conducted on the sandstone. During the initial studies, sedimentology and stratigraphy were the basis of all the research conducted. In 1976, Nijman and Nio interpreted the Roda as a complex of shelf sand and wave deposits (Nijman & Nio, 1975). In 1984, Nio then altered his interpretation to resemble an ebb tidal environment (Nio, Siengenthaler, & Yang, 1984). A year later in 1985, a team lead by Puigdefàbregas concluded that a tide-reworked fan delta most accurately represents the depositional environment of the Roda Sandstone (Puigdefabregas, Samso, Serra-Kiel, & Tosquella, 1985). Today, the most accepted interpretation is that the Roda is a wave-reworked delta, which was described by Crumeyrolle in 1992 (Crumeyrolle, Lesueur , Claude, & Joseph , 1992).

The Roda Formation is a unit composed of a mixture of clastic and carbonate sediments that have infilled the central section along the northern margin of the Tremp-Graus Basin. The entire formation is bounded by

two basin-wide carbonate units, the La Puebla Limestone at the base, and the Morillo Limestone at the top. The sediment of the Roda sandstone is believed to have been sourced from a granite pluton to the northeast of the study area. As the granite pluton was eroded, the sediment was transported towards the southwest along a paleovalley, where it was then deposited within the basin (López-Blanco, Marzo, & Muñoz, 2003).

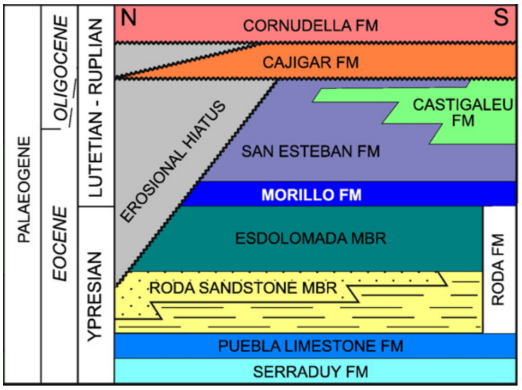

Figure 4: Stratigraphic section of the Isabena Valley (Leren, Howell, Enge, & Martinius, 2010).

The lower Roda Sandstone Member can be separated into six sandstone parasequences. These sandstone bodies are labeled Roda U-Z. The Roda sandstone was deposited in a Gilbert type delta system, with each of the Roda units representing a prograding sand lobe. As these sand lobes prograde basinward, they merge into calcareous mudstones (López-Blanco, Marzo, & Muñoz, 2003). During times of regression, the sand lobes prograde basinward. During transgression, a layer of well cemented carbonate sand is deposited. These carbonate deposits are found between the major sand lobes (Coll, López-Blanco, Queralt, Ledo, & Marcuello, 2013).

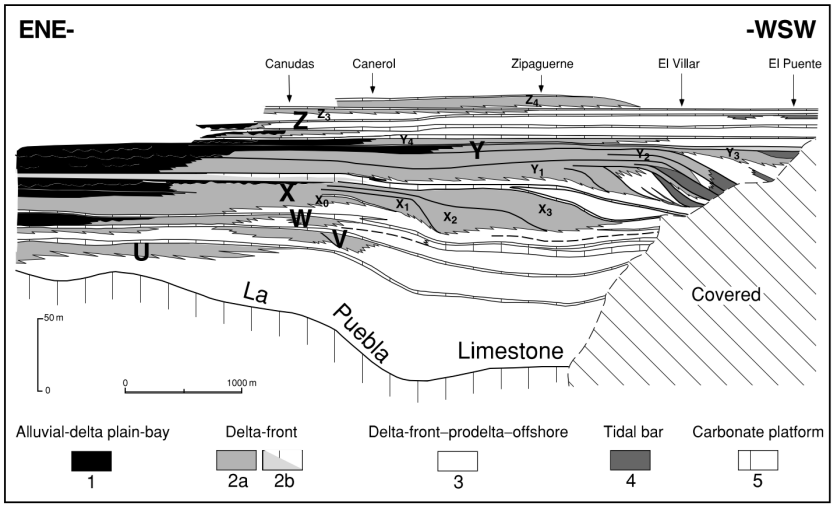

Figure 5: Cross Section of the Roda Formation. Six sand units are identified and labeled Roda U-Z. Cross section moves from proximal (ENE) to distal (WNW). (López-Blanco, Marzo, & Muñoz, 2003)

As the basin filled and accommodation space decreased, the entire system avulsed towards the east. As a result, the youngest deposits associated with the Roda are found more eastward. The same situation is present with the overlying Esdolomada member, as decreasing accommodation space results in a major turn towards the east with a large fan delta building out in the direction of the village of Aren.

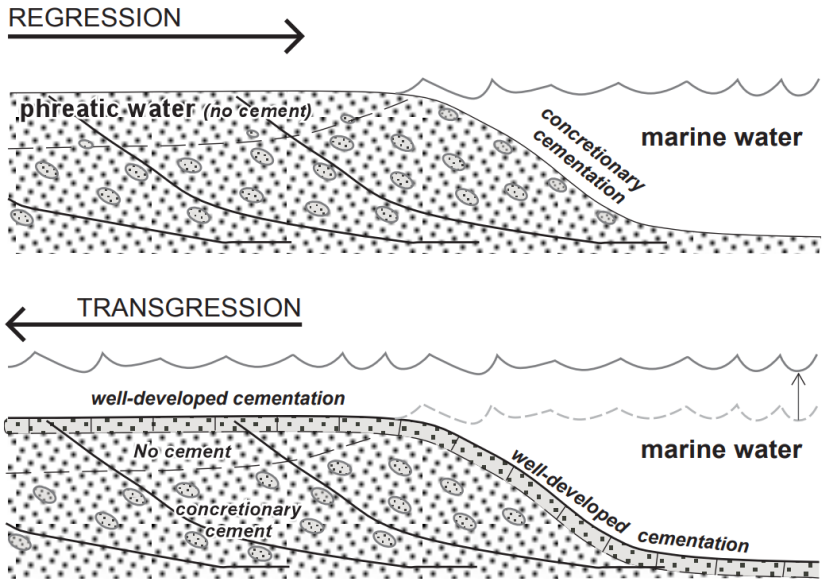

Figure 6: (Top) Creation of nodule cementation during times of low water level. (Bottom) Development of a well cemented carbonate layer on top of a sand lobe during transgression.

Tidal influence within the geological area involves tidal currents that are passed along the distal end of the fan delta but also turned into a morphological embayment created by the partly emergent fan delta itself on the eastern side and a partly emergent anticline located on the western side. This anticline, the Roda-Turbon anticline, was connected to structures that were part of the norther basin margin (López-Blanco, Marzo, & Muñoz, 2003). The resulting embayment enhanced the tidal currents and forced ebb and flood currents to follow the same path in and out of the embayment. Adapting this palaeogeographical situation and the associated hydrodynamic processes, including those forming the fan delta, will generate the most accurate model of the Roda Y sandstone due to input values derived from literature, as well as the data observed from the field samples. The accuracy of these models will tell us whether Delft3D can be utilized in these types of scenarios.

3.3 Processes Involved in Fan Deltas

When simulating a fan delta system, it is important to understand the processes involved during the transport and deposition of sediment within the system. These processes then have to be correctly incorporated within the process-based model.

A fan delta is formed when sediments from a river are deposited within a body of water (Seybold, Andrade, & Herrmann, 2007). These fan systems can be characterized by a steep gradient and fluvial systems displaying a conical shape. Fan deltas are highly influenced by climate and surrounding tectonics. Compared to river deltas, the reaction time of a fan delta is much quicker, due to the higher gradients of the river systems, as well as the relatively smaller drainage basins (Postma, 2003). The structure and shape of these deltas are dependent on the interaction between the source river and the basin in which the sediments are being deposited into. The river and basin can each have independent characteristics based on the surrounding ge-

ology and the combination of the two results in the unique structure of each individual fan delta. Factors controlling the river include climate, drainage area, sediment supply, as well as many others. The combination of these factors can result in one of two river systems, a braided river system, which includes a network of river channels with an abundance of braid bars and high sediment load, or a meandering system, which includes a much lower sediment load. The receiving basin also has a large influence on the shape of fan. The largest factor in fan architecture for basins is the gradient of the basin. Deltas being deposited in shallow water environments display a different shape than those that are deposited within a deep-water setting. Figure 7 displays the differences between the two environments. Tidal and wave factors can have an effect as they have the ability to rework the sediments post-deposition.

A Gilbert-Type delta is created when the ratio of river channel depth to basin depth is very low as well as containing a high bedload concentration (Postma, 2003). The resulting delta consists of a series of stacked prograding sand lobes, with each lobe displaying a coarsening upwards trend.

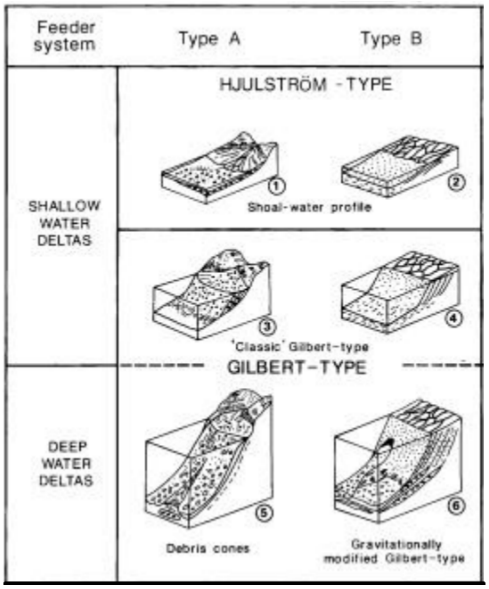

Figure 7: Shape and characteristics of shallow and deep-water fan environments. (Postma, 2003)

It is critical that these processes are correctly incorporated within the Delft3D simulations. Delft3D contains a large amount of input parameters which allows for the generation of a wide variety of models. There are a large number of factors in play and each must be respected and implemented to fully simulate the Gilbert-type delta system found in the South-Central Pyrenean Foreland Basin.

4 Spain Field Work

A trip to the Pyrenees Mountains in northern Spain took place to gather additional information about the Roda Sandstone. The location of the field work was the area surrounding the town of La Puebla de Roda, in the Province of Huesca. The Roda sandstone is distinctly outcropping throughout the valley and displays exceptional lateral continuity, resulting in a wide range of opportunities for data collection. The field work provided a better overall understanding of the system, as well as a hands-on analysis throughout different sections of the Roda Formation.

Figure 8: Overlook of the study area within the Isabena Valley, Northern Spain. (Michaud, 2011)

4.1 Methodology

4.1.1 Sample Collection

The purpose of this field work was to collect samples and their resulting grain size data that was later implemented into the process-based models. The grain size data was also used to check the calibration of the final simulations. The field work focused on different sections within the sand lobe. As a result, the samples provided a wide variety of grain size distribution data from different areas of the sand lobe. When combined, an overall grain size distribution for the entire system could be constructed. Samples from each location were collected from both the X and Y lobes. In total, 19 samples were collected, but only the 9 samples from the Y sand lobe will be analyzed due to time restrains in the lab and simulation run times. In future studies, the remaining samples from the Roda X can be utilized. The locations of the samples that will be used in the model are shown below in Figure 9.

Finding the boundary of the sand lobe required analyzing data available from literature detailing previous studies conducted on the Roda Sandstone. While some of the samples collected on the excursion were located in the boundary sections of the sand lobe, it was not possible to construct an overall outline of the sand lobe

based on this information, due to the uncertainties of the actual boundary edge of the lobe. Leren et. al. (2010) conducted an extensive study in the region that included a large number of sedimentological logs being taken throughout the area. They constructed an overall map for the Roda Y sandstone, outlining the overall shape of the lobe within the region. This map was used as a way to best estimate the location of the outer boundary of the sand lobe during the construction of our own map, in addition to our data collected from the field. Google Earth was used and an outline of the sand lobe was created using the measuring tool. It is important to note that the distal boundary of the lobe is not known, as it is located in the subsurface. The outline drawn below represents what is estimated to be the maximum extent of the lobe. It is a possibility that the boundary does not extent as far into the basin as what is depicted in Figure 9, which would result in a much smaller lobe. Sample collection was based on two primary aspects: the estimated location within the sand lobe, and the exposure of the outcrop.

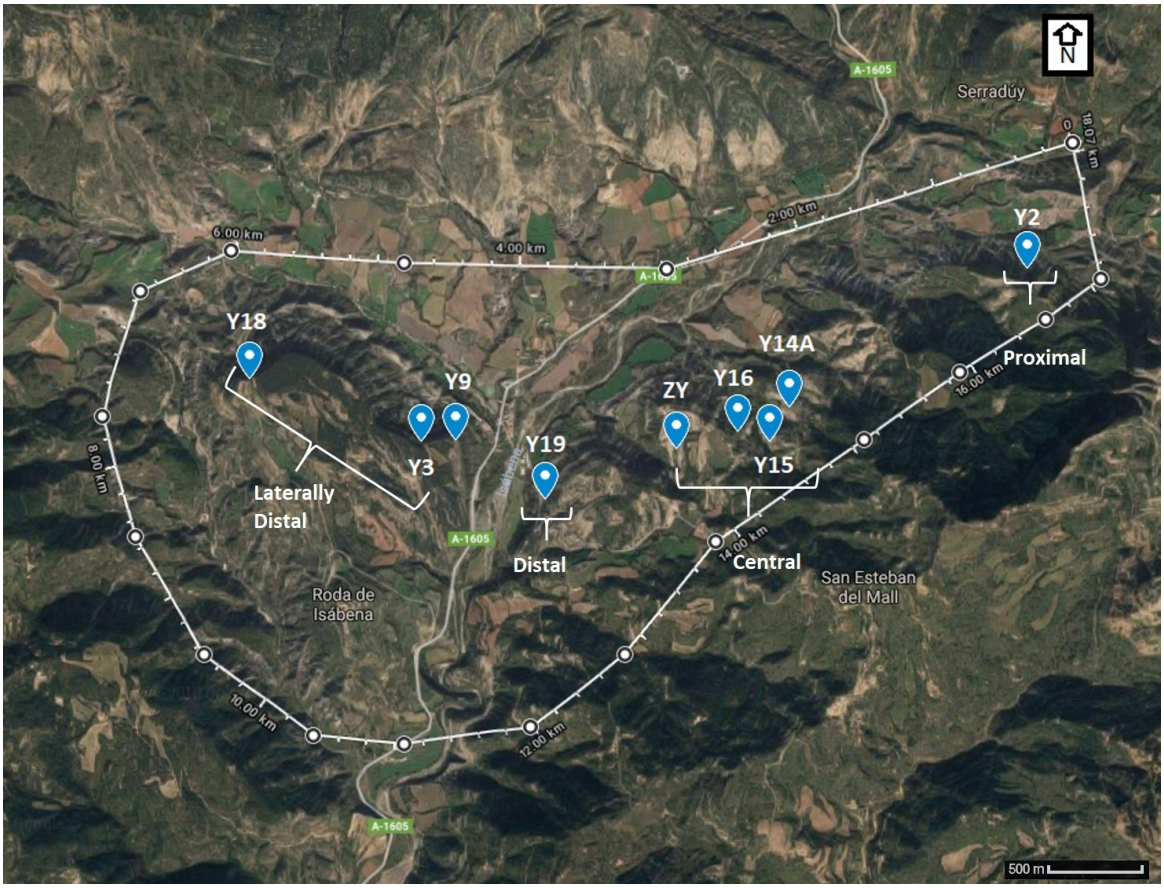

Figure 9: Map overview of the study area with sample locations and estimated outline of the Roda Sandstone.

4.1.1.1 Proximal The first sample to be collected was located in the proximal setting relative to the source. Sample Y2 was the only sample collected within the proximal setting. The location is approximately 1.2 kilometers to the south of the town of Serradúy. As the source is towards the northeast, the outcrop was chosen as it is one of the last accessible outcrops containing the Roda X and Y sand bodies as you move towards the northeast. It was also the location in which Leren et. al (2010) constructed sedimentological logs of the outcrop. These logs were used to ensure measurements are taken from the target unit, as the close stacking of the proximal deposits made it difficult to distinguish the different lobes.

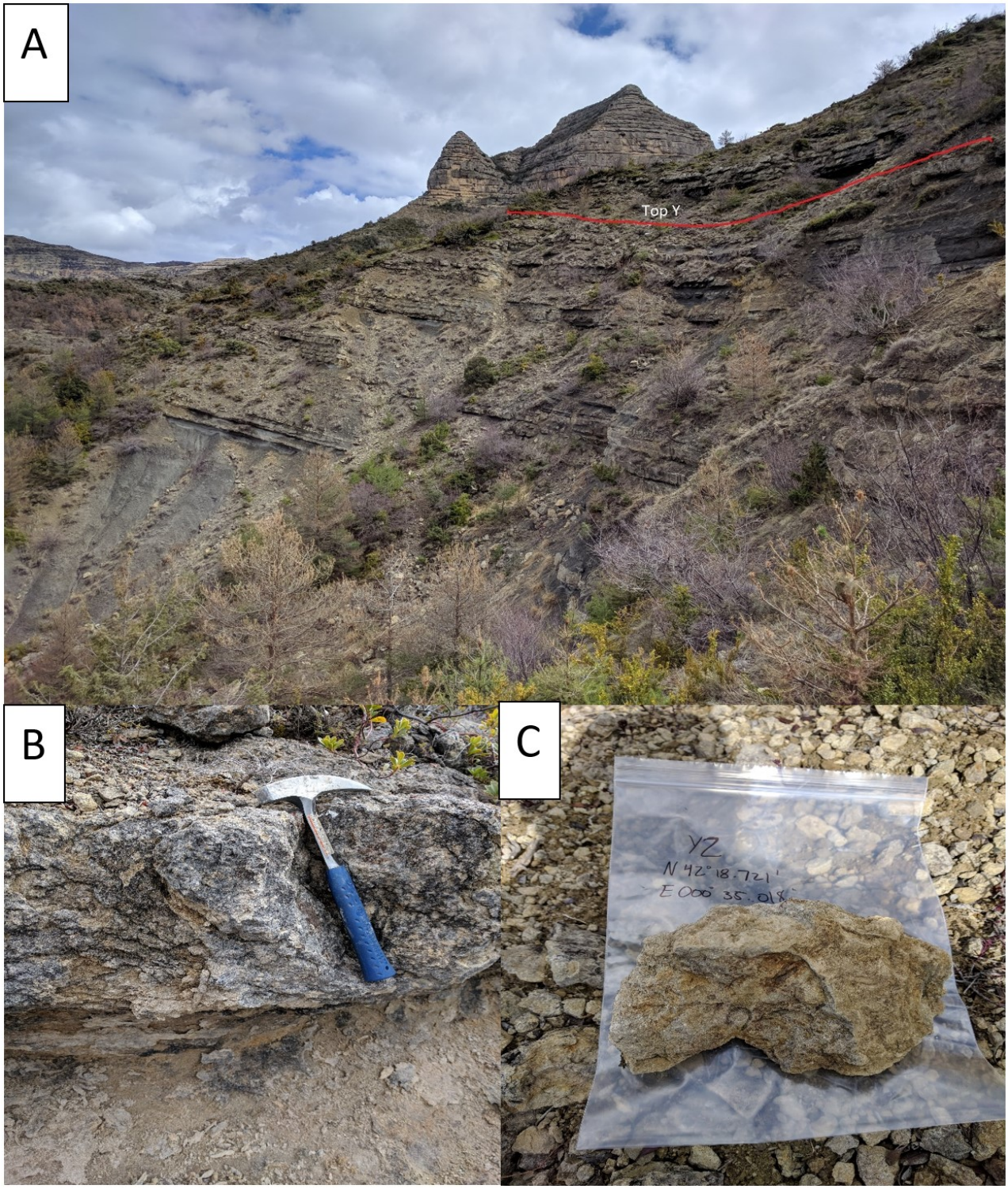

Figure 10: (A) Close stacking of sand lobes in the proximal setting. Top of the Y lobe is indicated by the red line. Location of sample collected is to the right of the view of the image. (B) Outcrop of which sample was collected. Large amounts of nodules are present, indicating high amounts of bioturbation. Length of hammer is 30.5 centimeters. (C) Sample collected from location. Large amounts of shell fragments found within the sample.

4.1.1.2 Laterally Distal The next location in which samples were collected was along the lateral edges of the lobe. These samples were collected from the outcrop located to the southwest of the town of La Puebla de Roda. Three samples from this location will be used in the model, with each being collected from different areas within the distal section of the lobe. Sample Y9 is the least laterally distal between the three samples, while sample Y3 is found roughly 230 meters west of sample Y9, in a more laterally distal section. The final sample, Y18, is located towards the west at the very edge of the sand lobe. The Roda Y is traced laterally along the outcrop until this point where the lobe can no longer be found. These 3 samples will provide the ability to study how grain size trends change even within a small area.

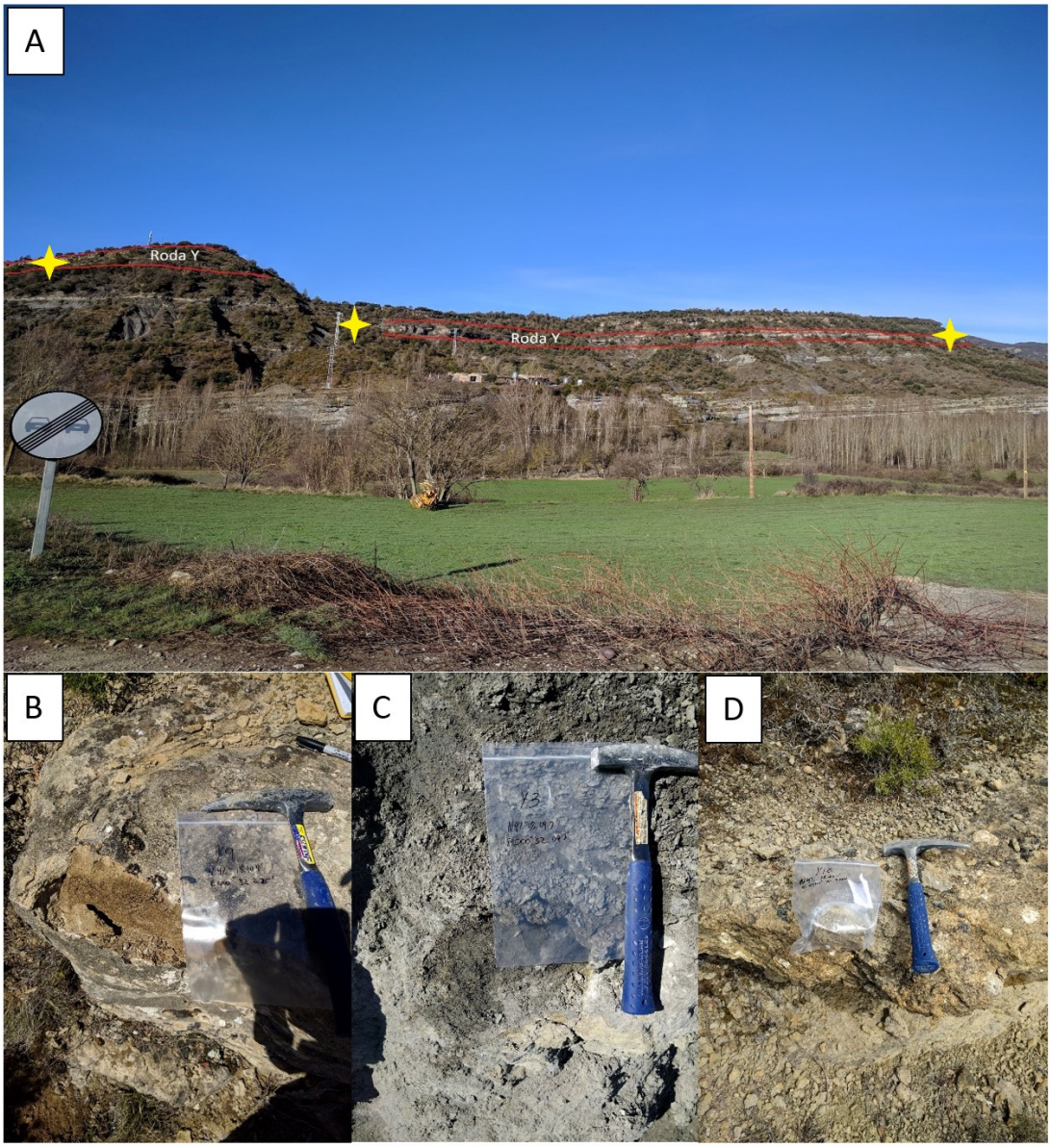

Figure 11: (A) Outcrop of laterally distal Roda Y deposits. Looking towards the southwest. The left star indicates sample Y9, while the middle star represents sample Y3. The right star is the location of sample Y18. (B) Location of sample Y9. Sample collected at the top of Roda Y sandstone. Length of hammer is 30.5 centimeters. (C) Location of sample Y3. Sample was collected from the base of the Roda Y. (D) Location of sample Y18. Most laterally distal of the three samples.

4.1.1.3 Central Lobe The third location where samples were collected was located in the central section of the Roda Y sand lobe. Four samples were collected from this location that were utilized within the model. From most proximal to distal, the samples collected were Y14A, Y15, Y16, and ZY. Samples Y14A and Y15 were collected from the base of the Y sand lobe. In this location, it was clear to see the Roda Y sandstone overlaying the highly dipping Roda X. A fine-grained carbonate layer is present between the Roda X and Roda Y.

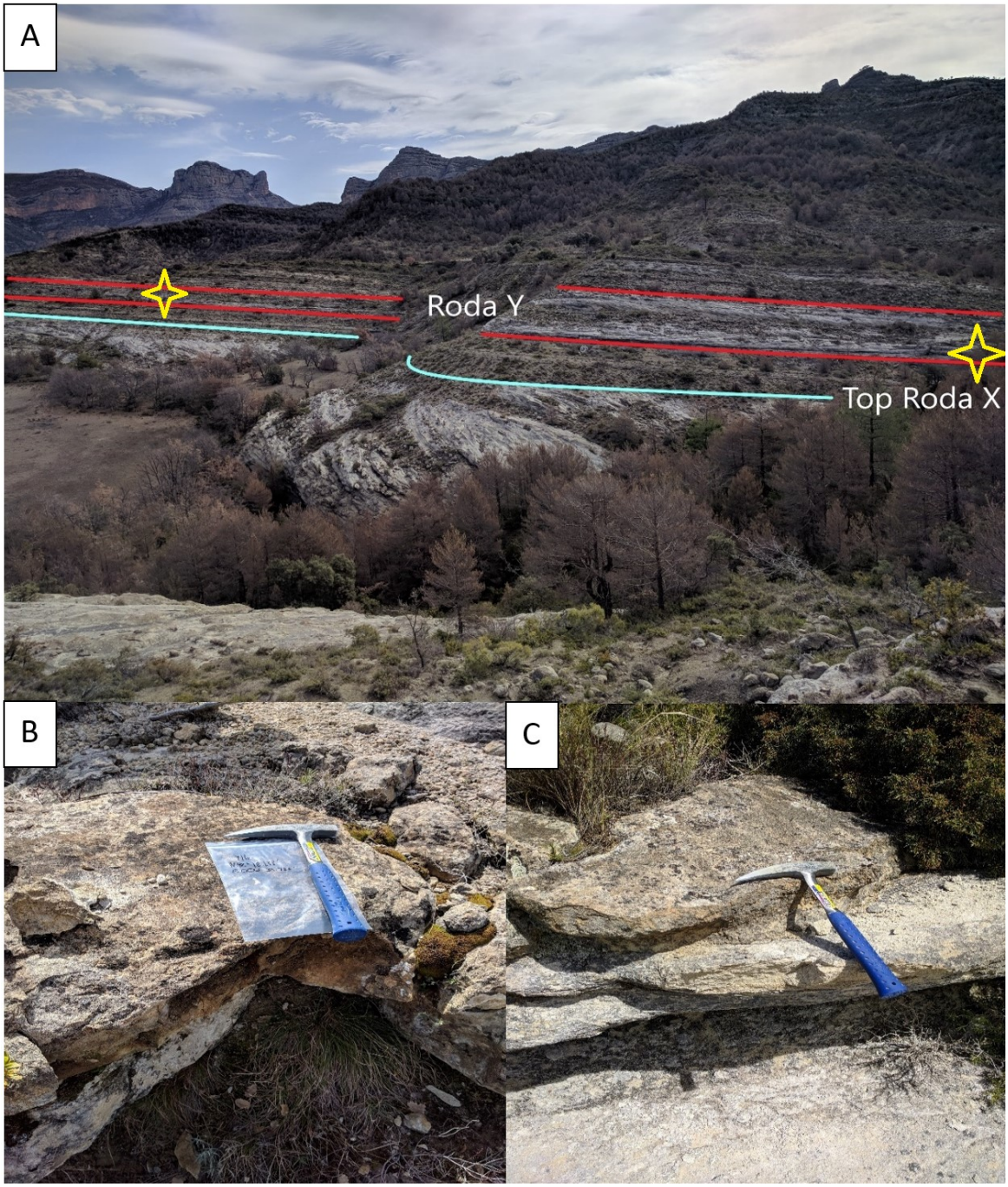

Figure 12: (A) Overlook of central lobe location. Looking in a northeastern direction. Left star indicates location of sample Y14A. Right star indicates location of sample Y15. (B) Outcrop of sample Y16. Collected at base of Roda Y. Length of hammer is 30.5 centimeters. (C) Outcrop of ZY sample. Sample ZY is the most southern of the centrally collected samples.

4.1.1.4 Distal With the Roda Y sandstone exhibiting a southward dipping trend, the outcrop eventually submerges into the subsurface. It is not known how much further the sand deposit continues in the subsurface past the last visible outcrop point, but is estimated to be roughly 1000 meters. It is at this last outcrop point that the final sample was collected. This represents the most distal measurement from the source. This sample is located approximately 3.75 kilometers to the southeast of the sample collected in the proximal area. While sample Y19 is the most distal sample collected, it is important to remember that this does not necessarily represent the absolute distal edge of the sand lobe, as the lobe continues towards the southwest in the subsurface.

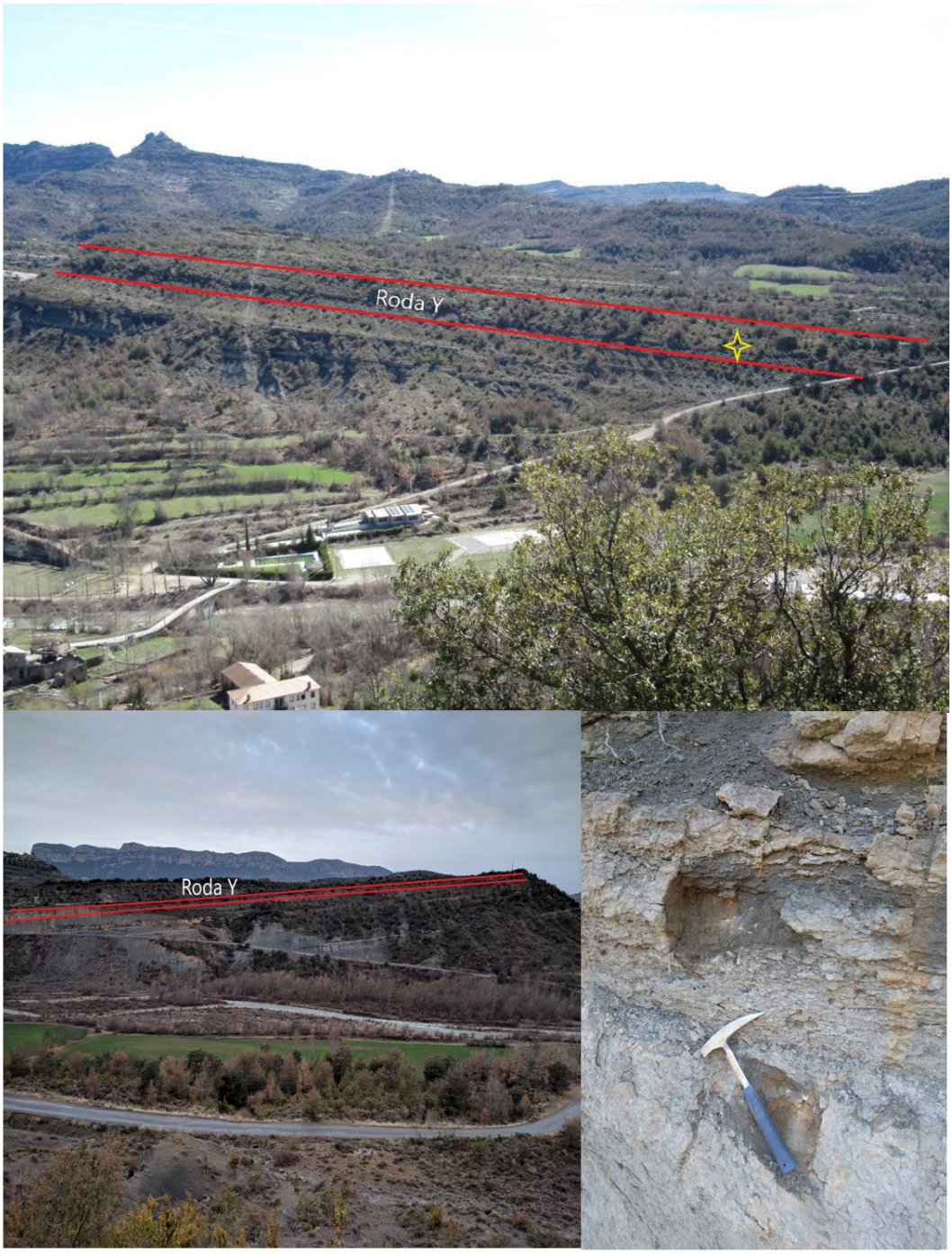

Figure 13: (A) Location of sample Y19, represented as a yellow star. Picture was taken across the valley, facing towards the east. (B) Southward dipping Roda Y sandstone, facing west from the location of sample Y19. (C) Location in which sample Y19 was collected. Length of hammer is 30.5 centimeters.

4.1.2 Creation of Thin Sections

Once the samples were collected and transported back to Delft, a grain size analysis was performed on each sample. Thin sections were created for each of the 9 samples and analyzed for sediment composition and grain size. Images of each sample were taken and analyzed within the program Leica Qwin (Version 3.2.1, 2005). Figure 14 below shows an example of sample ZY after it was made into a thin section.

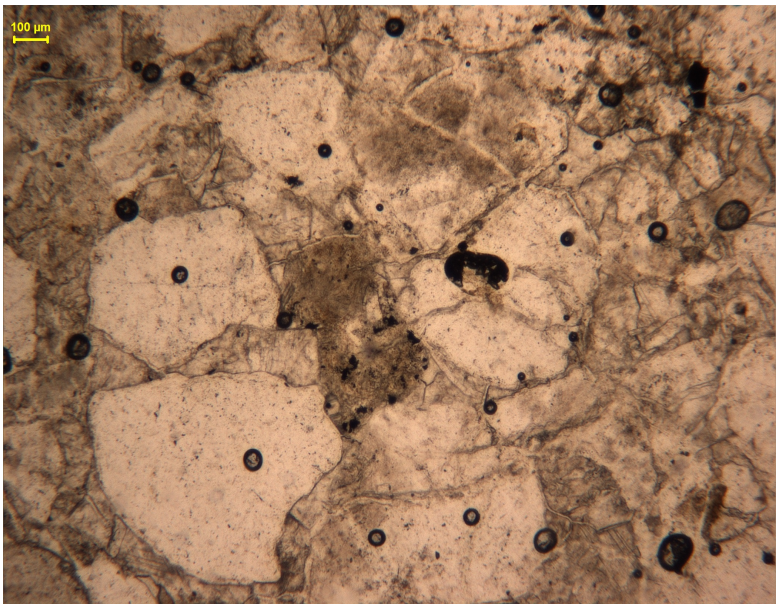

Figure 14: Image of sample ZY under 4X magnification.

The analysis was performed by measuring the grains present in each image. The resulting data was transferred to excel to be analyzed and sorted. An average of 8 pictures per sample were taken throughout different areas of the thin section to ensure that the data points depict an accurate representation of the entire sample. The total measured distance from end to end for each of the grains was added up and divided by the amount of grains present to give the overall grain size distribution of the sample. The grain sizes were assigned categories, which can be found below in Table 1 (Wentworth, 1922).

Table 1: Grain size categories and equivalent measurements

Grain Size Class	Grain Size (μm)
Coarse	1000-500
Medium	500-250
Fine	250-125
Very Fine	125-62.5
Mud	<62.5

4.1.3 Interpolation of Data

After the grain size analysis was performed, the grain size distribution over the entire sand lobe was calculated. Within Delft3D, grain size parameters, such as grain size, density, concentration, and many others, are input values for each of the sediment classes present. To ensure the generation of the most accurate model possible, it is critical that the concentrations of different grain sizes are as accurate as possible to what is observed in the outcrop data.

An interpolation was performed over the entire sand lobe to generate the concentrations of each grain size class. For the interpolation, the application "QUICKIN" within Delft3D was used and the triangular interpolation process was utilized. The first step involved plotting the grain size distributions for each of the nine samples on a generated grid. The grid is identical to the one used within the simulations, and a single grid cell contains a dimension of 50x50 meters. The samples were placed in locations on the grid that represent their location in the real-world setting, as well as accurate spacing between each sample. The boundary of the sand lobe was estimated based off of literature and field observations. Points were added in the grid along the edges of the sand lobe to act as a boundary for the interpolation, as well as to ensure that the entire sand lobe is being interpolated. These additional points along the edge were assigned values similar to those of sample Y18, which was collected at the edge of the sand lobe. Each grain size was interpolated over the entire system based on the grain size ratio for each sample. In total, 5 different interpolations were generated to represent each of the 5 different grain sizes present. Sample locations and additional locations on the grid for fine grained sediment are shown below in Figure 15.

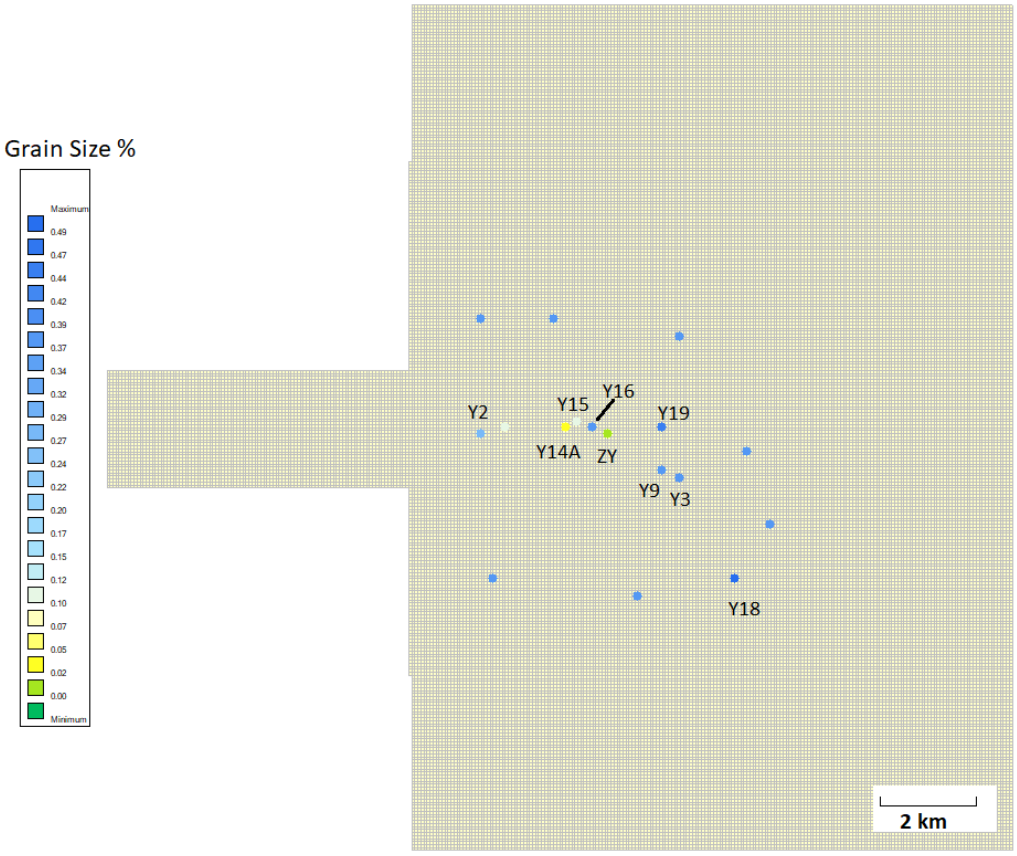

Figure 15: Relative locations of samples collected from the field, as well as the addition of points added along the edge of the lobe. Points not labeled are points which were added manually. Data points are representative of fine grained sediment.

With a grain size distribution for the sand lobe constructed, it was now possible to calculate the concentrations for each grain size class. The first step involved combining the data that was generated from the five interpolations. The result of the triangular interpolation produced a list of X and Y coordinates for the grid over the entire area, and the corresponding percentage for each grain size class. The grain size percentages were averaged over the whole area, which results in a single value representing the percentage of that grain size in the entire sand lobe. This process was performed for each of the five grain size classes.

Once the grain size distribution for the Roda Y sandstone has been constructed, the next step is to calculate the total amount of sediment present for the sand lobe. The methodology in this step involved finding the rough area of the lobe and then multiplying this value by the thickness of the sand lobe.

With the outline shown above in Figure 9, the area is calculated to be 16.67 km^2. With the total area calculated, the average thickness was calculated. The thickness of the Roda Y Sandstone varies from a couple meters thick, and upwards of 30 meters in some locations (Leren, Howell, Enge, & Martinius, 2010). Leren et. al. (2010) indicates an average thickness of roughly 20 meters over the entire sand lobe. While we did not take any thickness measurements in the field, we did not observe 20 meter thick successions of sand, especially in the distal

locations. Therefore, the average thickness chosen for this calculation was 15 meters. This value incorporates the data we witnessed in the field, but still taking into consideration of the higher number of samples measured from Leren et. al. (2010).

With the area and average thickness known, the total volume of sand was calculated along with the corresponding grain size concentration for each sample. Multiplying the area, 16,670 square meters, with an average thickness of 15 meters, results in 250,050 cubic meters of sediment. A total sediment load concentration of 0.15 kg/m^3 is used for sediment input, based on measurements from modern delta systems ((Milliman & Farnsworth, 2011). The mud concentration is entered as 0.05 kg/m^3, as there is not an easy way to estimate the amount of mud initially, as the majority of the mud will be washed into more distal sections and are only preserved at the sample locations in limited quantities. This value was varied in each of the simulations. With the mud concentration having a value of 0.05 kg/m^3, the remaining sediments have a combined concentration of 0.1 kg/m^3.

The previously found percentages of each grain size found through the interpolation technique were multiplied by the remaining overall concentration, 0.1 kg/m^3. This process was performed for the coarse, medium, and fined grained sediments. To account for the presence of carbonate within the very fine sediment, the concentration had to be scaled for the difference in densities. For sand, a value of 1,600 kg/m^3 is used, and for carbonate sand, a value of 1,700 kg/m^3 (Trautmann, Kulhawy, & O'Rourke, 1985). The percentage of very fine-grained sand was split in two, with the concentration of sand assigned a density of 1600 kg/m^3, while the remaining percentage was assigned the carbonate density, 1700 kg/m^3. With carbonate being 1.06 times denser than sand, the carbonate concentration of 0.01 was multiplied by 1.06, as well as the sand concentration of 0.02 being divided by 1.06. The resulting concentrations now include the roughly 10% carbonate composition.

4.2 Results

The data from the samples are vital to the overall success of the project as they act as the base parameters for the final simulations. This section conveys the results of the experiments conducted on the samples collected from the Roda Y sandstone in Spain.

4.2.1 Grain Size Distribution per Sample

The first step involved obtaining grain size distributions for each of the nine samples collected. With this data, overall trends were interpreted for the entire system. A petrography analysis was performed on the samples as well, with the findings showing roughly a 10% composition of very fine-grained carbonate sand, which is similar to what is found within literature (Molenaar, 1990). The samples were categorized based on the location of sampling within the sand lobe, and the resulting grain size distributions for each sample are shown in the sections below.

4.2.1.1 Proximal Only a single sample, Y2, was collected from the proximal setting. The location of the of sample is located southwest of the ancient river mouth. Within this sample, 392 grains were measured and analyzed. The results are shown below in Figure 16.

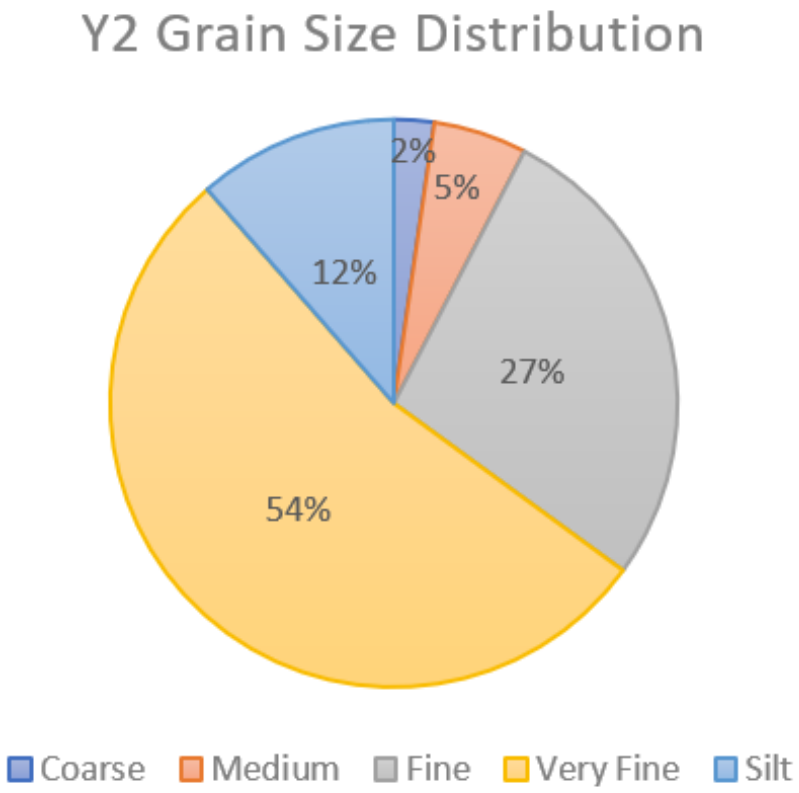

Figure 16: Grain size distribution, based on number of grains present, of sample Y2.

The distribution exhibits a very fine-grained trend, as very fine grained material makes up 54% of the overall composition, while medium and coarse grained sand has a combined percentage of 7'%. The sample was collected from the base of the sand lobe.

4.2.1.2 Central Lobe Within the central location of the lobe, four samples were collected, Y14A, Y15, Y16, and ZY. There is a spacing of roughly 250 meters between each of the samples. Sample 14A is closest to the source, based on the what is believed to be the location of the source, with the other samples increase in distance from the source, moving towards the southwest (Leren, Howell, Enge, & Martinius, 2010). The grain size distribution for the four samples can be found below in Figure 17.

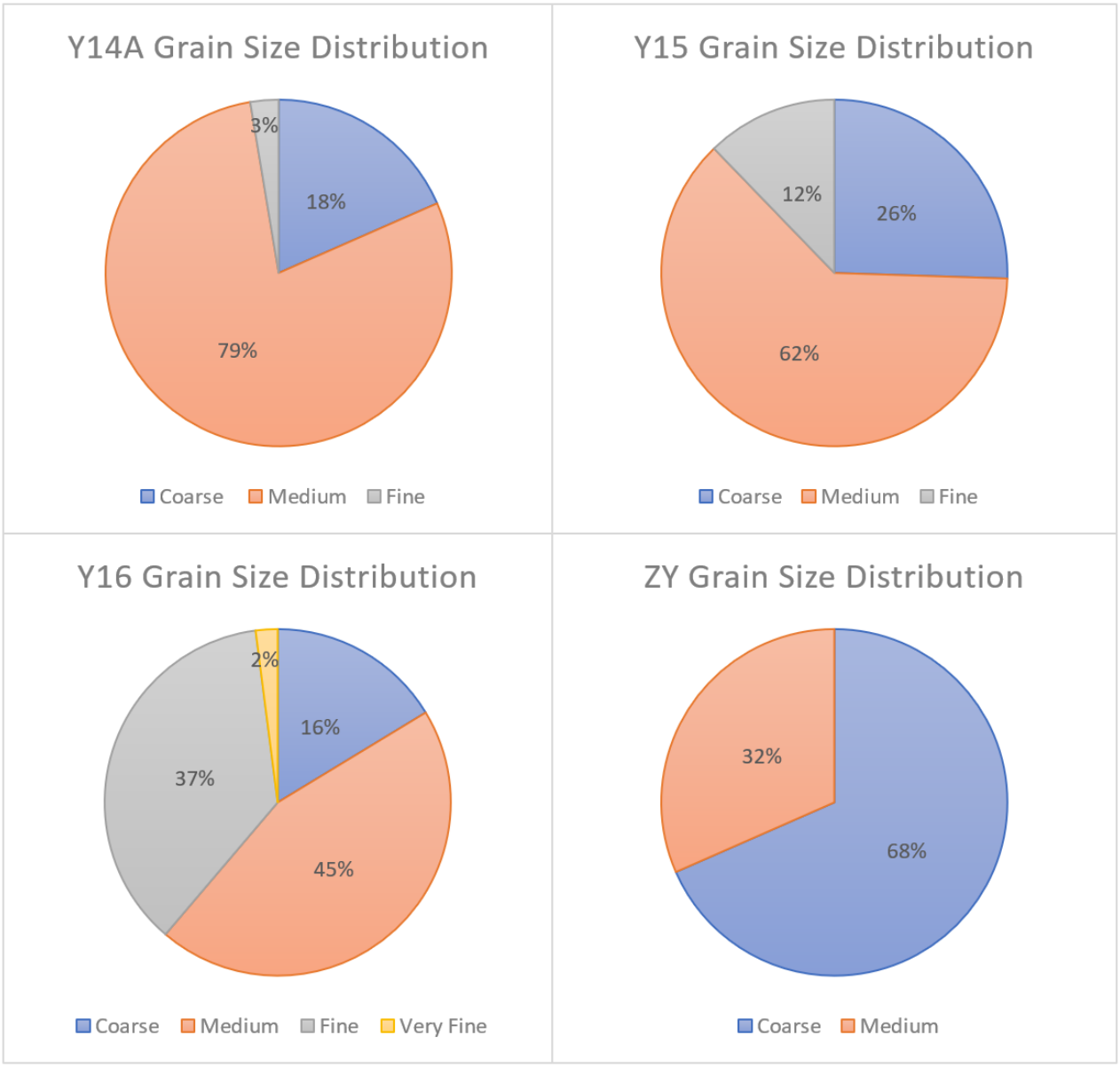

Figure 17: Grain size distribution, based on number of grains present, for four samples collected from the central lobe location of the Roda Y sandstone.

As shown in the figure above, the central area of the sand lobe contains the highest concentration of medium and coarse-grained sediments. As these coarser grained sediments enter the basin, the resulting loss in water energy deposits them before they can extend further into the basin (Russell, 1968)

4.2.1.3 Distal Four different samples were collected in different distal sections of the lobe. Samples Y3 and Y9 were collected in a lateral distal section, only 25 meters apart. Sample Y18 was collected at the distal edge of the sand lobe. This is the location in which the Roda Y can no longer be seen beyond the sample location. Sample Y19 was collected at the most distal section of the lobe before it dips into the subsurface. This is the furthest point measurable from the ancient river mouth. The results are shown below in Figure 18.

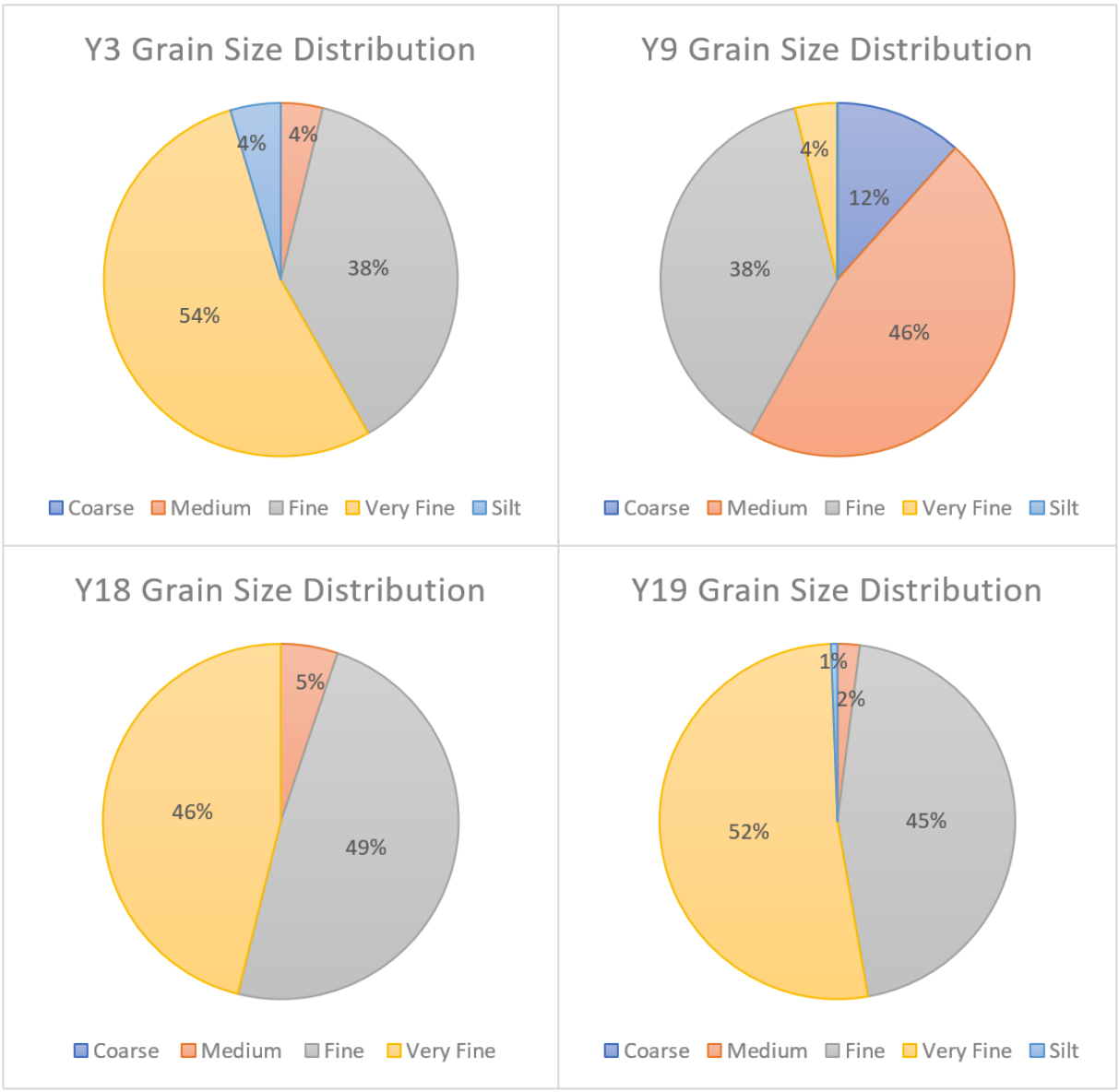

Figure 18: Grain size distribution, based on number of grains present, for four samples located in the distal sections of the Roda Y sandstone.

When comparing the grain size distributions shown above, sample Y9 acts as an outlier compared to the other distal samples. One possible explanation for this could be the position in the outcrop that the sample was collected. Sample Y9 was collected at the very top of the Roda Y sandstone, as opposed to sample Y3 being collected at the base. The entire system displays a coarsening upward trend, so this observation fits with the overall grain size model, but the large variance to a sample in close proximity is questionable.

Delft3D requires each sediment input to have a mean sediment diameter. With the data collected from the thin section analysis, the measured length of each grain was put into grain size categories for the entire group of samples. The average grain size was then measured for each of the measured grain size classes. The results are shown below in Table 2.

Table 2: Average measured grain size for each grain size class, taken from sampels collected from the Roda Y sandstone.

Grain Size Class	Grain Size (μm)
Coarse	657
Medium	357
Fine	163
Very Fine	98
Mud	51

4.3 Analysis of Results

With the results from the thin section analysis complete, it was now possible to analyze the final grain size distributions for the sand lobe. As discussed in section 5.1.3, the known grain size percentages for each grain size class were plotted and interpolated over the entire area. Figure 19 shows the interpolation of the 4 grain size classes for sand.

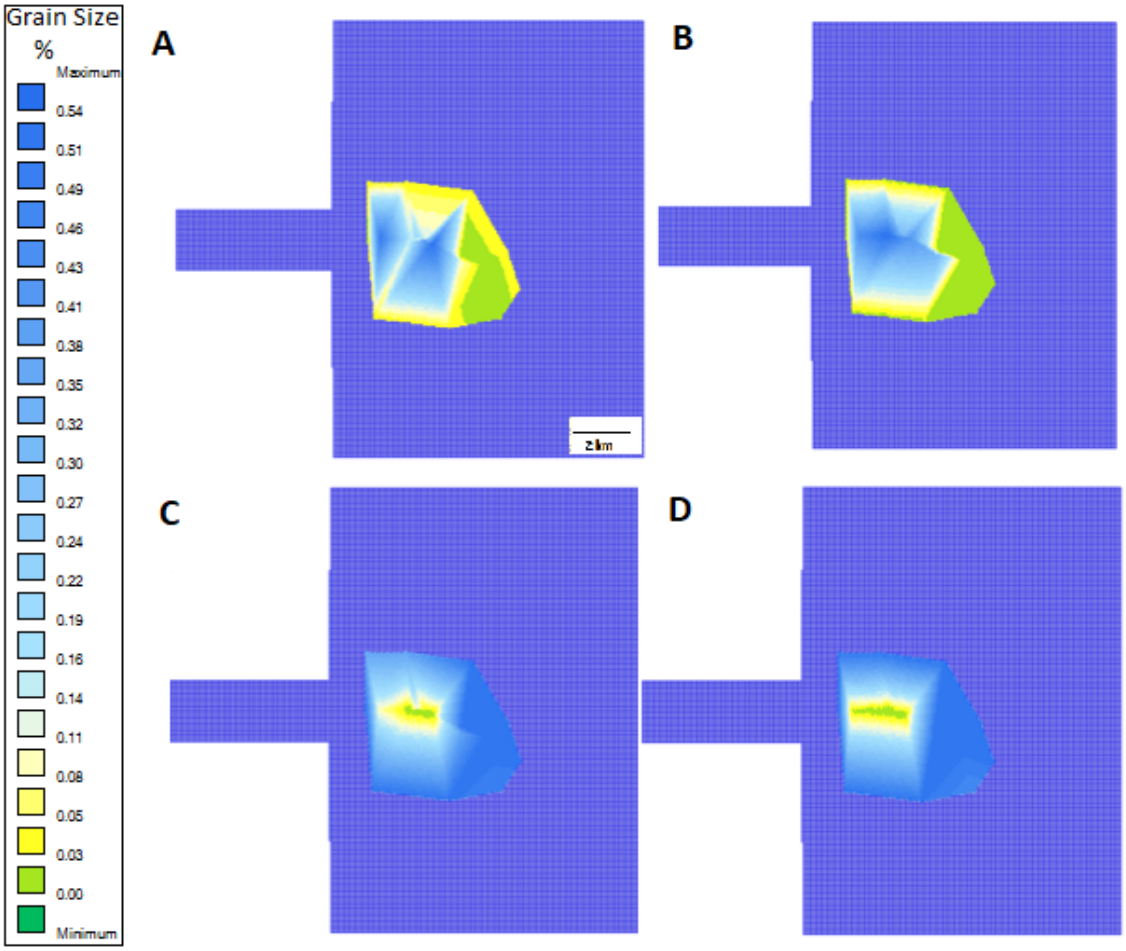

Figure 19: Interpolation for (A) coarse, (B) medium, (C) fine, and (D) very fine grained sediment. Dark blue colors indicate high concentrations while green and yellow colors indicate low concentrations. Scale is constant throughout the four interpolations.

As shown in the figure, the finer grains are found at the distal edges of the lobe, while the central section

contains the coarser grained material. The interpolations show that the laterally distal sections, while still containing predominately fine-grained material, contain a higher percentage of coarser material than compared to the distal sections. Fine-grained percentages average around 14% to 30% in the lateral sections, while distal sections range from 40% to 50%.

The results for the grain size interpolation over the entire system, based on the averaging of each grain size class, are shown below in Figure 20.

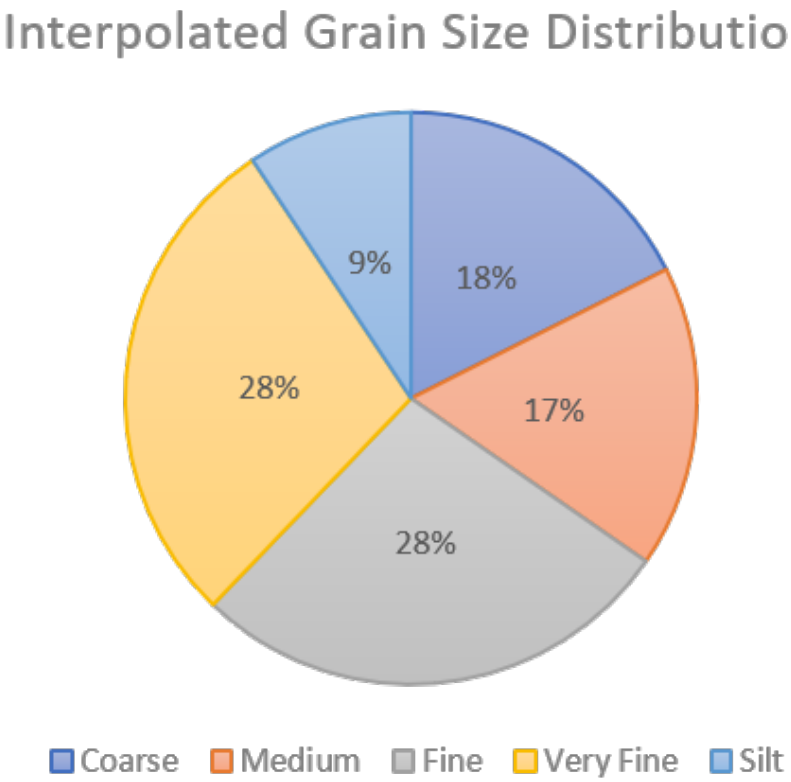

Figure 20: Grain size distribution for the Roda Y sandstone based off of triangular interpolation within Delft3D.

Very fine and fine-grained material make up the majority of the distribution, but the coarse material still represent a significant portion of the grain size distribution. Coarse grained material represents 18% of the entire system, while medium grained sediment represents 17%. Mud contains 9% of the overall distribution. As a whole, this distribution represents the characteristics of a typical Gilbert-type delta, while accurately depicting the data collected from the field samples.

The final results are shown below in Table 3. These concentrations will act as the sediment input values for the simulations.

Table 3: Concentrations for each of the four grain size classes, including the addition of carbonate into the system.

Grain Size Class	Concentration (kg/m^3)
Coarse	0.0185
Medium	0.0180
Fine	0.0290
Very Fine Sand	0.0188
Very Fine Carbonate	0.0106

With the grain size distribution data collected from the analysis, a grain size map of the Roda Y sand lobe was constructed. The grain size interpolations for each grain size were combined to create a single map of the area. The results are shown below in Figure 21.

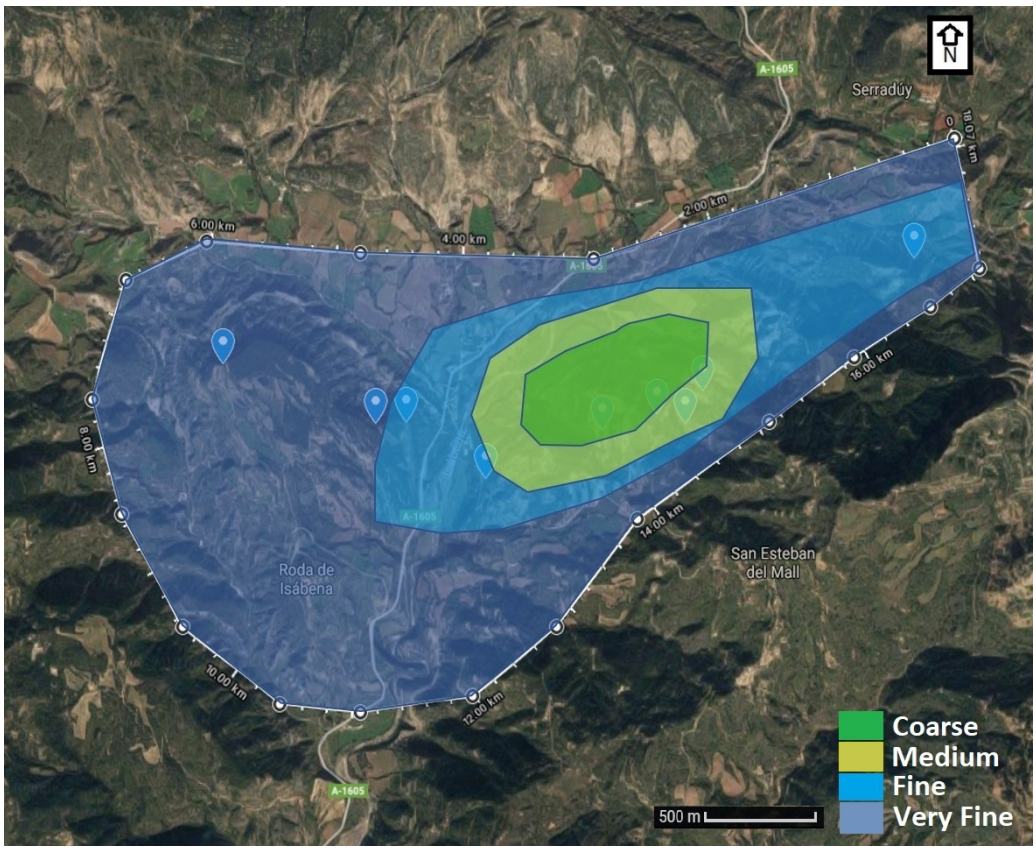

Figure 21: Grain size distribution over the Roda Y sandstone.

4.4 Discussion

The results from the the field data display the grain size distribution throughout the sand lobe. Nine samples were chosen from the field to be used within the experiment. The spacing between the locations in which the samples were collected allows for a large sample area that incorporates the different locations within the sand lobe.

The results of the grain size distribution indicate a system which is composed of predominately fine and very fine grained sediments, but each sample contains a different grain size distribution based on the location of the

sample within the sand lobe. In the most proximal setting, sample Y2 contains approximately 54% very fine grained sand and 27% fine grained sand. For a proximal setting that typically contains high amounts of energy due to the proximity of the source, one might expect to find coarser grained material. The vertical location of the sample within the unit greatly affects the grain size distribution. The Roda Sandstone displays a coarsening upwards trend in each of the sand lobes (Yang & Nio, 1989). Sample Y2 was collected from the base of the Roda Y sand lobe, therefore it represents the finest grained material present in this location. The thickness of the lobe at this location is approximately five meters, therefore it is not expected that the grain size does not change substantially in such a small succession. Leren et. al. (2010) observed a predominately medium grained sandstone in a location that is roughly 10 meters from the location of our sample.

Within the central region of the lobe, four samples were collected, all from varying locations vertically within the succession. The results of all four samples show a distribution that is medium and coarse grained. This represents a location of high energy during deposition (Russell, 1968). Sample ZY was taken at the top of the Roda Y sand lobe, and contains the highest percentage of coarse grains. While the coarsening upward trend is still present in this location, the change is much lower than what is observed in other locations. This could be caused by the amount of energy present throughout deposition. Due to the central location of the lobe, the variation in energy remained low throughout deposition

The distal sections of the lobe are composed of very fine and fine grained sand. Small amounts of mud are found as well, upwards of 12%. The availability of sample locations in the distal sections of the lobe is low, and as a result, additional points were added manually to form the boundary of the lobe. When analyzing the result, it is important to keep this factor in mind. The boundary of the lobe, and how far it extends into the basin, was based off of literature and the resulting model simulations may extend further, or may not reach the interpolation boundaries. This will have to be accounted for in the analysis of the simulation results.

The results of the interpolations must be respected in that they do not represent what is found in the subsurface. The interpolations tend to be more basic in that they do not incorporate structural aspects of the sand lobe, such as channels. The creation of channels and their affect on the distribution of sediments plays a large part in how different sediments are transported and deposited (Hubbard, Covault, Fildani, & Romans, 2014). The interpolations still provide a reasonable representation of the grain size distribution for each grain size class over the entire sand lobe.

Future work in the field could focus on the change in grain size over small areas. This could include measuring grain size trends vertically in each sample location, as well as the locations around the sample to measure the change horizontally. This could provide useful information on grain size distribution on a small scale, and how large of a factor the location of the sample plays on the resulting data. Would collecting a sample a couple meters to the left have a profound affect on the overall grain size distribution? A further analysis could help answer this question.

5 Simulations

Deltares' program "Delft3D" was used to run all of the simulations. A total of five simulations were run, each with varying input parameters. The sediment input parameters were gathered from the thin section analysis of the samples collected from the Roda Sandstone. Delft3D incorporates sediment transport and erosional forces during the simulations. This results in sediment being deposited, and possibly eroded away as the simulation moves forward. Within Delft3D, the "FLOW" application was used to run the simulations. FLOW incorporates many hydrodynamic factors, including tides, waves, and other aspects of the depositional and erosional processes. 5 simulations were chosen due to the amount of run time required for each simulation, as well as to not overload the server that is running the simulations. If time allowed, additional simulations would have been run and analyzed.

The purpose of the running the simulations was to see if process-based models could replicate the results found from the grain size analysis. Five simulations were run, each with a parameter that was altered to observe how each variable can affect the outcome of the model. The main objective was to find a set of input parameters such that the grain size distribution of the simulation matches the approximate distribution of the field data interpolations as closely as possible. Another objective is to match the shape and geometry of the lobe. Gilbert-Type deltas exhibit prograding sand lobes stacked upon one another (Ferrer-Boix, Martín-Vide, & Parker, 2015). The lobe geometry is much different than a river-dominated delta, such as the Mississippi River. An ideal result would be a model that matches the shape and size of the Roda Y Sandstone.

5.1 Methodology

5.1.1 Model Input Parameters

The input parameters used in the simulations were derived from literature and are kept constant throughout all of the simulations. They act as the conditions associated with the basin, such as bathymetry and other aspects. Each simulation then used a variety of sediment input values that were slightly altered for each simulation.

One of the most important aspects when dealing with a Gilbert-type delta is the topography and slope of the basin. Gilbert-type deltas are generated when a river empties coarse grained sediment into a relatively steep deep marine basin. The basins are typically highly sloping (Gobo, 2014). These Gilbert-type deltas are common within areas with high tectonic activity, such as the South Pyrenean Foreland Basin.

In the case of the Roda sandstone, the bathymetry is different for each of the sand lobes. In the case of the initial Roda U sandstone, the sediments were deposited along the initial basin slope. Initially, there was adequate accommodation space at the proximal areas. As Roda V started to be deposited after Roda U, there was little accommodation space at the proximal areas. As a result, a thin layer of sediment is deposited on the underlying unit. The unit has to prograde deeper into the basin to reach higher accommodation space, which results in thicker deposits (Martinius, 2017). The Roda Y sand lobe has roughly 1000 meters of alluvial-delta

plain before reaching delta front deposits. To account for this, the bathymetry was created in that there is a series of step-downs, with the first step-down being adequate distance from the river mouth, as opposed to a gradual continual slope. This represents the previous stacking of prograding sand lobes. The river mouth in these scenarios is approximately 950 meters wide. In the real-world case, the tides move parallel to the coast line, and as a result, they push the sediment towards the south-west. This causes the sand lobe to move towards the south-west as it is deposited. Since it was not possible to replicate this tidal situation within Delft3D in the time available, the bathymetry was modified so that the basin is sloping from east to west. The slope is less than 1 degree, to favor a southwestern lobe orientation.

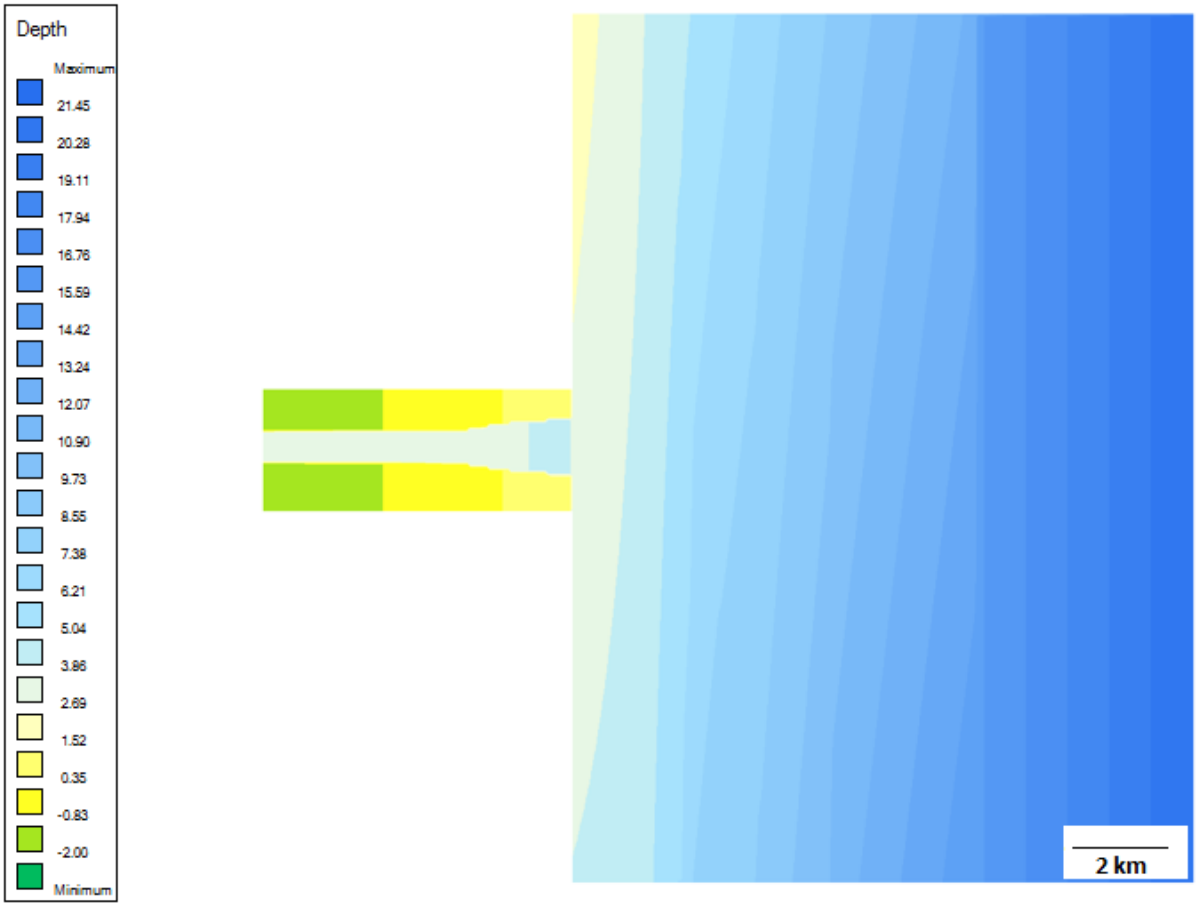

Figure 22: Modelled bathymetry of the Tremp-Graus basin after deposition of Roda X sand lobe. Positive numbers indicate depth below the surface, while negative numbers indicate elevation above sea level.

When constructing the grid, precision and computational time were taken into account. The goal was to construct a grid that was as detailed as possible, that could also be computed in a reasonable time. A grid of 50 x 50 meters was chosen. This is as precise as possible while still maintaining acceptable computing time.

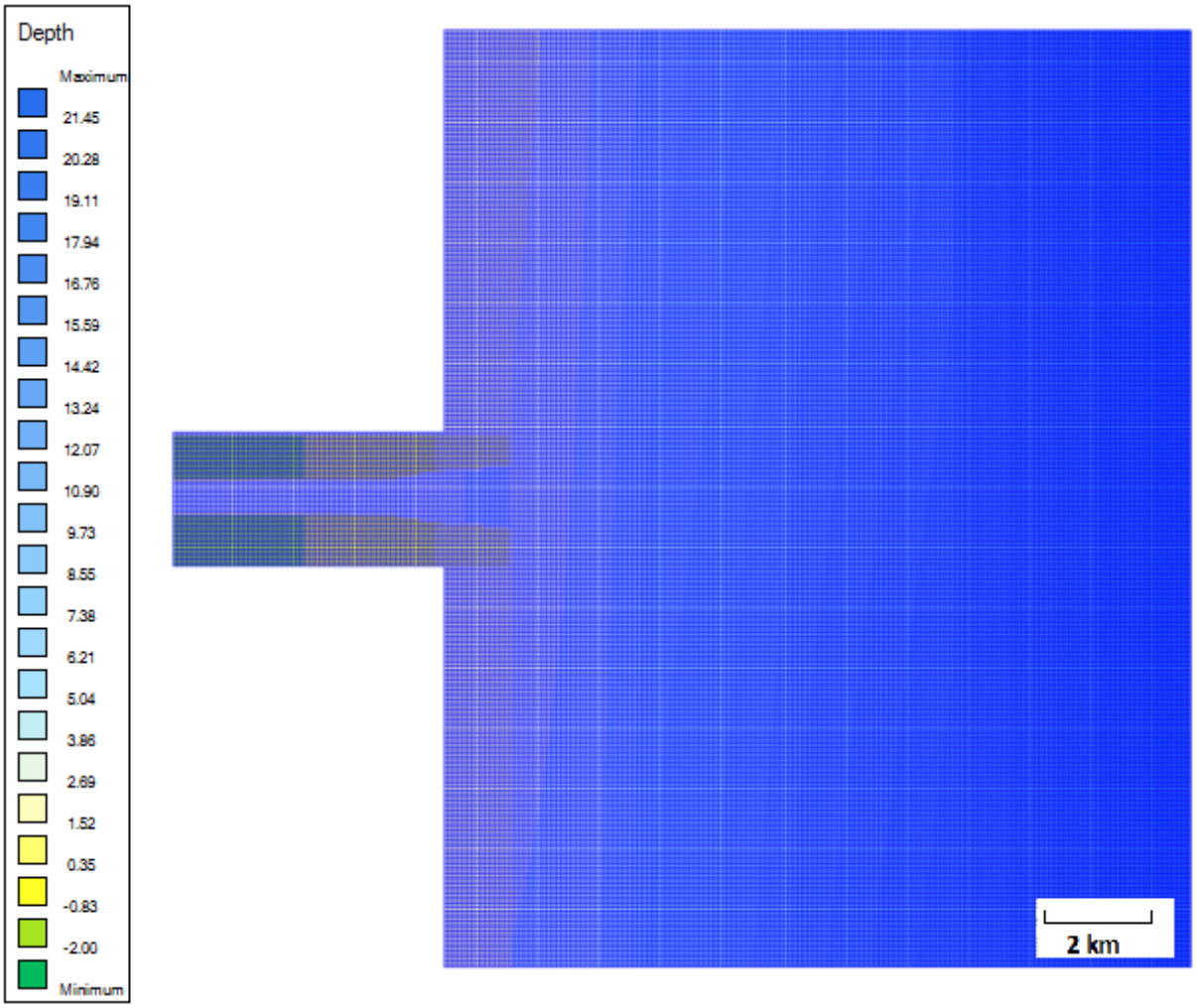

Figure 23: Grid overlying the bathymetry of the Tremp-Graus Basin.Positive numbers indicate depth depth below sea level. Negative numbers indicate elevation above sea level.

The entire grid has a dimension of 204 x 208 cells. This represents a space of 10,200 x 14,000 meters. The size of the grid and basin allow for the sediment to have ample space to settle under normal conditions, without reaching or being affected by the boundaries.

In the real-world scenario, tides ran parallel along the coast from the East to the West. In the simulations, this was not taken into account due to the complexity of adding this tidal structure. In this case, the tides entered from the basin, and moved perpendicular to the shoreline into the embayment along the toe of the fan delta. The tides then returned in the same direction they originated from. The two boundaries perpendicular to the shoreline are given open Neumann conditions, which allows sediment to exit outside of the boundaries

A hydrodynamic time of 321 days was given as the time frame for the flow module. The wave, tidal, and fluvial boundary conditions of the model are set to operate under this time frame. To scale up the simulation, a morphological factor of 30 was selected. As a result, 1 hydrodynamic year represents 30 years of deposition and erosion. A hydrodynamic time of 321 was chosen through analysis of past simulations. This time period allows for the sand lobe to reach a size that is similar to the Roda Y sand lobe.

Within Delft3D, there are a variety of sediment transport and deposition formulas that can be utilized. Two of the most commonly used formulae are the default Van Rijn transport formula and the Engelund-Hansen formula. The Engelund-Hansen formula was chosen as it reflects the total transport, as well as allowing the compartmentalization of bedload and suspended load, each of which can be calculated individually (van der Vegt, 2018). When incorporating this formula, each grain size is categorized into a specific grain size value (D50) for non-cohesive sediments and settling velocity and critical shear stress for erosion for cohesive sediment.

For the simulations, the following conditions were kept constant:

Table 4: conditions kept constant throughout all of the simulations.

River Mouth	950 meters
River Discharge	1500 m^3/s
Basin Slope	1 degree
Wave Height	0.5 meters
Timestep	1

The simulations were run based on the sedimentological data collected from the thin section analysis. Each simulation varied from the previous one while keeping the main sediment composition and concentration the same. Small aspects were changed in each model to observe the affect it has on the final result. Table 5 below displays the sediment parameters for each of the five simulations.

Table 5: Sediment input parameters for all simulations. * indicates simulations in which the critical bed shear stress for erosion (TcEro) was increased from 0.12 N/m^2 to 0.3 N/m^2. The following sections explain the reasoning behind the values that were chosen.

	Coarse	Medium	Fine	Very Fine (Sand)	Very Fine (Carbonate)	Mud
Grain Size (μm)	657	357	163	98	98	51
Density	2600	2600	2600	2600	2700	2650
	Concentration (kg/m^3)					
Simulation 1	0.0185	0.0180	0.0290	0.0188	0.0106	0.0500
Simulation 2	0.0185	0.0180	0.0290	0.0188	0.0106	0.0800
Simulation 3	0.0185	0.0180	0.0290	0.0300	0	0.0800
Simulation 4*	0.0185	0.0180	0.0290	0.0188	0.0106	0.0500
Simulation 5	0.0185	0.0180	0.0290	0.0188	0.0106	0.0147

5.1.2 Simulation 1

The first simulation that was run included the sedimentological data that was collected from the thin section analysis. In this model, the amount of mud is increased from that which is observed within the sample. The total amount of mud thought to be within the system is hard to estimate based off of measured data due to the probability of the majority of mud that was initially deposited being eroded and washed away. With this in mind, the mud concentration was increased to 0.05 kg/m^3, up from 0.015 kg/m^3.

5.1.3 Simulation 2

Simulation 2 is very similar to simulation 1 as the sand and carbonate concentrations are kept the same. In this simulation, the mud concentration is increased from 0.05 kg/m^3 to 0.0800 kg/m^3. As stated before, it is difficult to correctly gauge the amount of mud present within the system due to erosion, this increase will help cover the possibility of a higher mud concentration within the delta.

5.1.4 Simulation 3

The third simulation that was run was to focus on the effect that the presence of carbonate has on the system. Carbonate makes up roughly 10% of the entire composition of the Roda Y sandstone, so it is beneficial to see how the difference in density affects the system. In this scenario, the presence of calcite is removed. The concentration associated with the calcite will be added to the very find sand concentration, due to the similar grain sizes. The mud concentration from Simulation 1, 0.050 kg/m^3, is used in this simulation.

5.1.5 Simulation 4

The previous three simulations modified the sediment composition and concentrations to observe the effects on the system, Simulation 4 will modify the parameters regarding erosion within the delta. The critical bed shear stress for erosion (TcEro) was increased, from 0.12 N/m^2 to 0.3 N/m^2. The TcEro affects the ability of the cohesive mud to be eroded. A higher TcEro will allow lower degrees of erosion, which can affect the creation and migration of channels within a delta. This can lead to drastic changes for the shape and architecture of the sand lobe as the way sediment reaches the outer edges of the delta is changed.

5.1.6 Simulation 5

The fifth model simulation that was run was using the mud concentration found in the thin sections. The previous models accounted for situations in which additional mud was added to the system, this simulation will account for the opposite and will provide a comparison of the two techniques. Simulation 1 has a mud concentration of 0.0500 kg/m^3, while a concentration of only 0.014 kg/m^3 was found in the sample. The TcEro has been decreased to 0.12 N/m^2 so that it is identical to the previous simulations involving variations in mud concentration. This will result in a system in which only the mud concentrations are changed.

5.1.7 Analysis of Results

Once the simulations were complete, the next step was to analyze and compare the results. The goal was to compare the grain size distribution from the simulation with the interpolation from the thin section analysis. The difference between the model results and the interpolations gives a representation of how well calibrated the model is.

The simulations produced large data files that needed to be prepared before it can be used in the interpolations. MATLAB was used for the data preparation. Delft3D generates grain size distribution in a series of 77 bookkeeping layers. The first step was to read the grain size fraction of each of the 77 layers. The grain size distribution was taken at the first and the last time step. The next step involved reading the layer thickness for each of the 77 classes. The final bed thickness was neglected, as it is a 30-meter-thick base layer that was not deposited by the simulation. With the thickness of each layer defined, the thickness of each grain size class was calculated. The sediment present at the beginning of the simulation was subtracted from the simulation present at the end of the simulation, resulting in only the sediment deposited during the simulation. The thicknesses for each of the grain size classes were then summed together, resulting in the grain size distribution for each grain size over the entire sand lobe.

The results from the grain size interpolations were loaded into MATLAB for the five grain size classes. For each grain size class, the results from the simulation were subtracted from the interpolation results. This was performed for each grain size class. As the simulation produced more data points than present in the interpolation, only points that were present within both data sets were analyzed. The difference between the two data sets represents a total percent difference over the entire sand lobe for each grain size class. This process was performed for each of the five simulations. The MATLAB code used for the analysis can be found in Appendix D.

An additional process was performed to check the difference between the simulation results and the data observed from the field samples. Points within the simulation results were chosen that represent the location of each of the nine samples. The mean grain size was then calculated for each sample. Within each sample, the concentration of each grain size was multiplied by its corresponding phi value, which is based on the size of the grains. These values are then summed up to find the overall phi value for the sample. The equation to find the mean grain size of the sample is shown below.

$$D = D_0 * 2^{-\phi}$$

D represents grain diameter (mm), D_0 is the reference diameter, in this case it is 1 mm. The phi values associated with each grain size class are shown in the table below.

Table 6: Grain size classes and their corresponding phi values.

Grain Size	ϕ
Coarse	0.6
Medium	1.5
Fine	2.75
Very Fine	3.4
Mud	4.1

This process acts as a way to check the calibration at each of the nine samples, as well as specific locations within the generated sand lobe.

5.2 Results

This section conveys the results of each of the five simulations, as well as the comparison to the interpolated and sample data. These results will show an indication of how well each of the five models is calibrated to match the real-world data.

5.2.1 Geometry of Sand Lobe

Each of the five simulations generated sand lobes that have a unique shape and structure. The sand lobes for each of the five simulations are shown below.

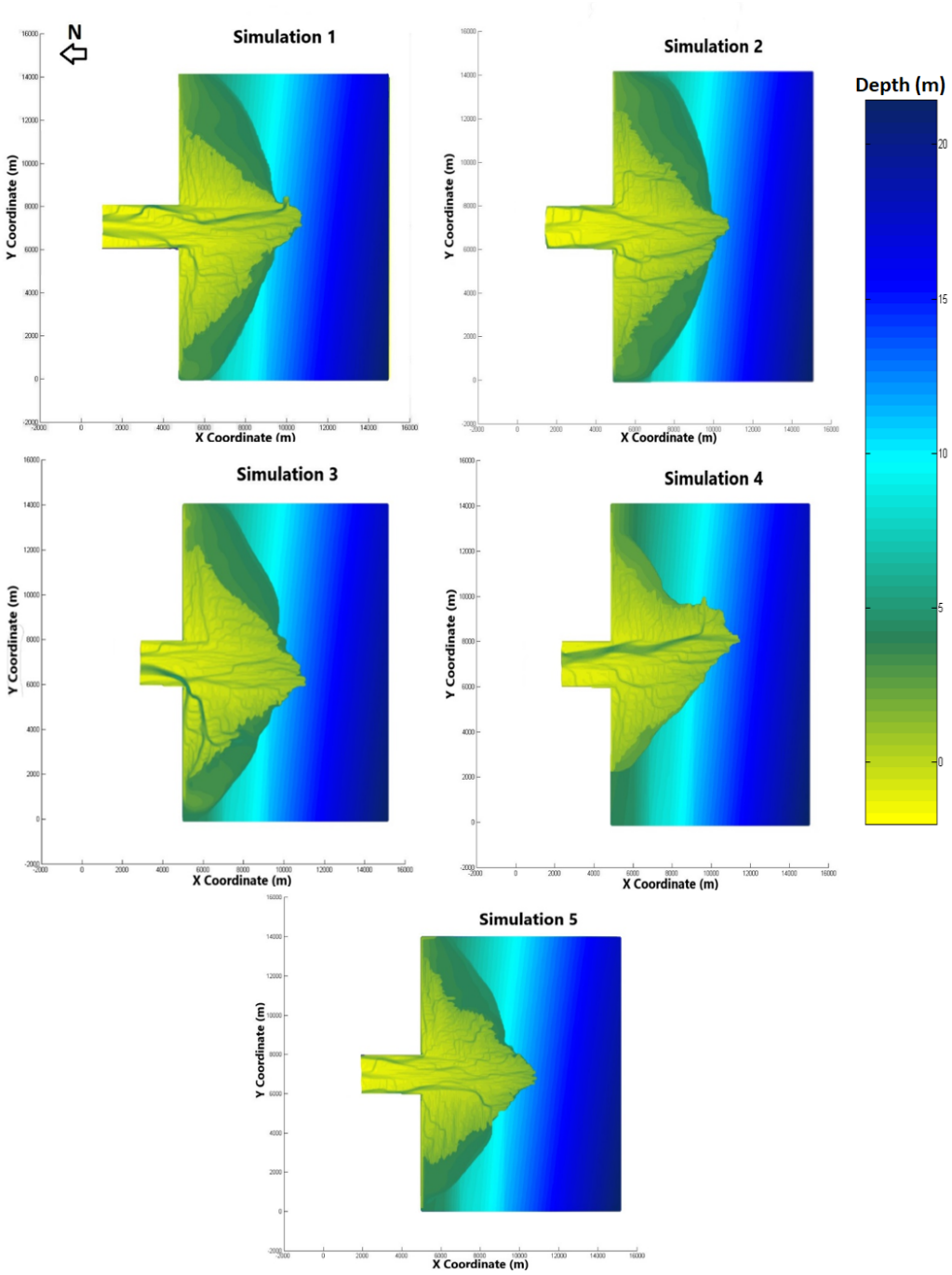

Figure 24: Final shape of the sand lobe for each of the five simulations. Images were collected after timestep 321.

5.2.2 Grain Size Distribution

The grain size distribution of the sand lobe is heavily dependent on the sample location within the lobe. Figure 25 below displays the mass of each grain size class deposited within the sand lobe for the five simulations.

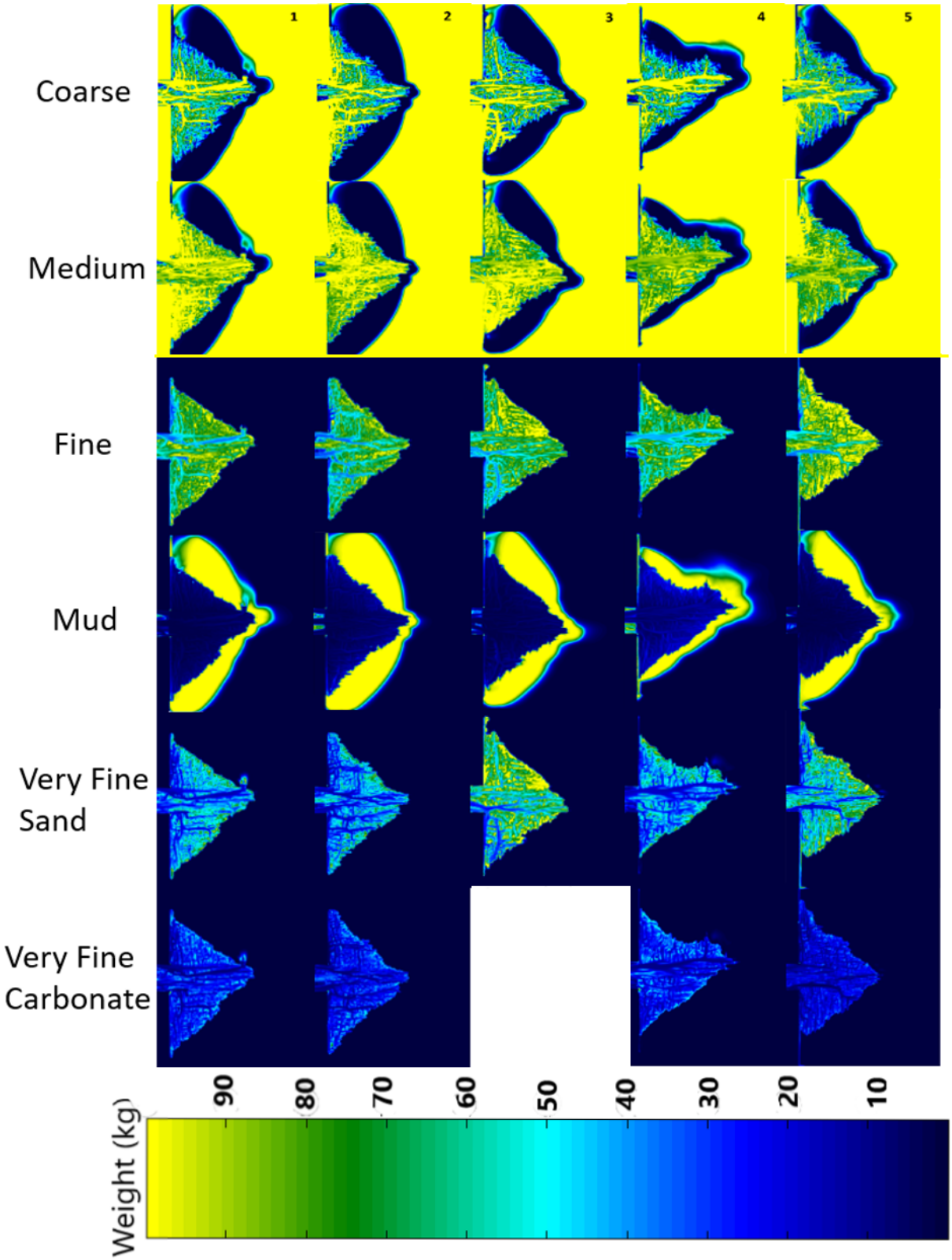

Figure 25: Sediment weight deposited for each grain size class in each of the five simulations. Columns are labeled 1-5 with the corresponding simulation. In Simulation 3, only one very fine grain size class is present.

For each simulation, the results of the of the model were subtracted from the interpolation data for each grain size class. This results in a percentage of the difference between the simulations, and the real-world data. The results for each of the five simulations are shown below. Negative values indicate higher percentages in simulation data.

5.2.3 Simulation 1

Table 7: Average percent difference between the interpolation data and the simulation results for each grain size class from Simulation 1. Negative values indicate higher percentages in the simulations.

	Coarse	Medium	Fine	Very Fine	Mud
Average	5%	5%	20%	21%	-10%

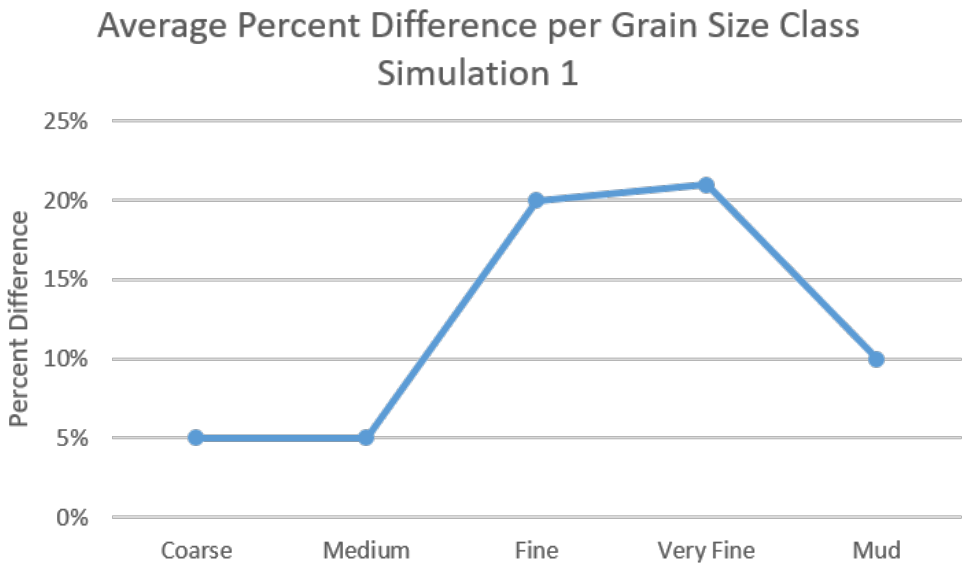

Figure 26: Average percent difference between interpolation and model results for each grain size class in Simulation 1.

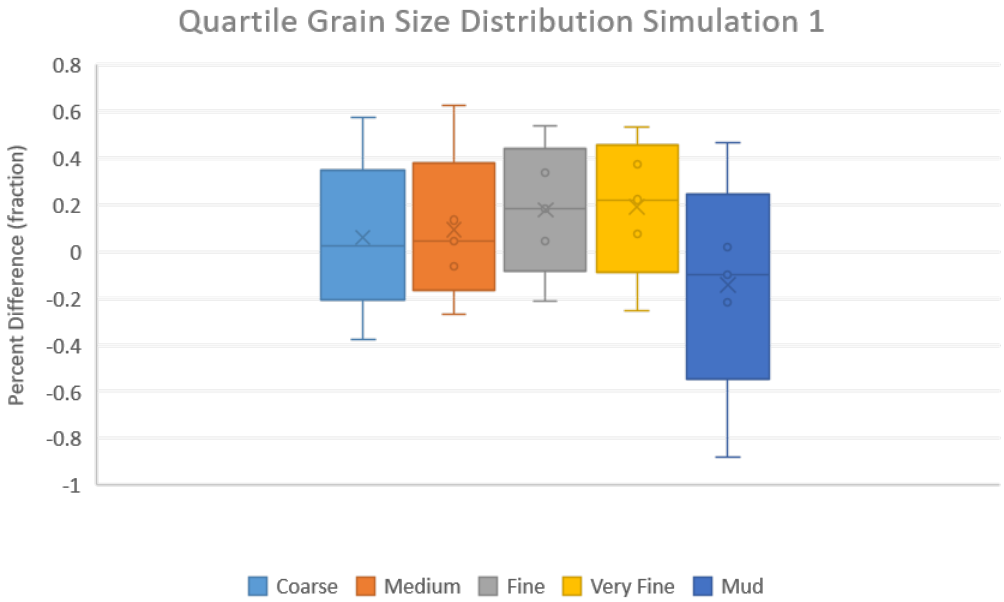

Figure 27: Quartile grain size distribution for the five grain size classes for Simulation 1. "X" indicates mean value. Graph indicates range of values present, therefor values do not sum to 100.

As shown above in Figure 26, the average difference for coarse and medium grained sand is low, 5% for both grain size classes. The average percent difference sharply rises for fine and very fine sediment, an average of 20% and 21%. When analyzing Figure 27 above, it is apparent that while coarse and medium sized grains contain a lower average, the spread of values is higher than that of the fine and very fine grains. The mud class contains the highest spread of values of all the grain size classes. When analyzing Figure 25 above, the sand lobe extends approximately 6 kilometers into the basin, and roughly 4 kilometers laterally on both sides of the river mouth. A noticeable prodelta extends at the edge of the sand lobe. Large channels can be found that run perpendicular to the shoreline.

5.2.4 Simulation 2

Simulation 2 increased the concentration of mud present within the system to 0.08 kg/m^3, up from 0.05 kg/m^3.

Table 8: Average percent difference between the interpolation data and the simulation results for each grain size class from Simulation 2. Negative values indicate higher percentages in the simulations.

	Coarse	Medium	Fine	Very Fine	Mud
Average	7%	7%	21%	22%	-18%

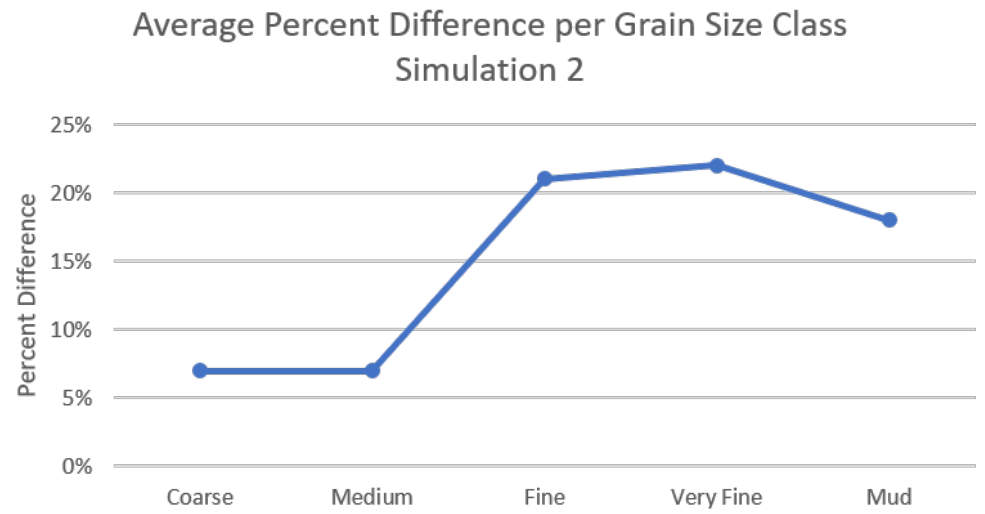

Figure 28: Average percent difference between interpolation and model results for each grain size class in Simulation 1.

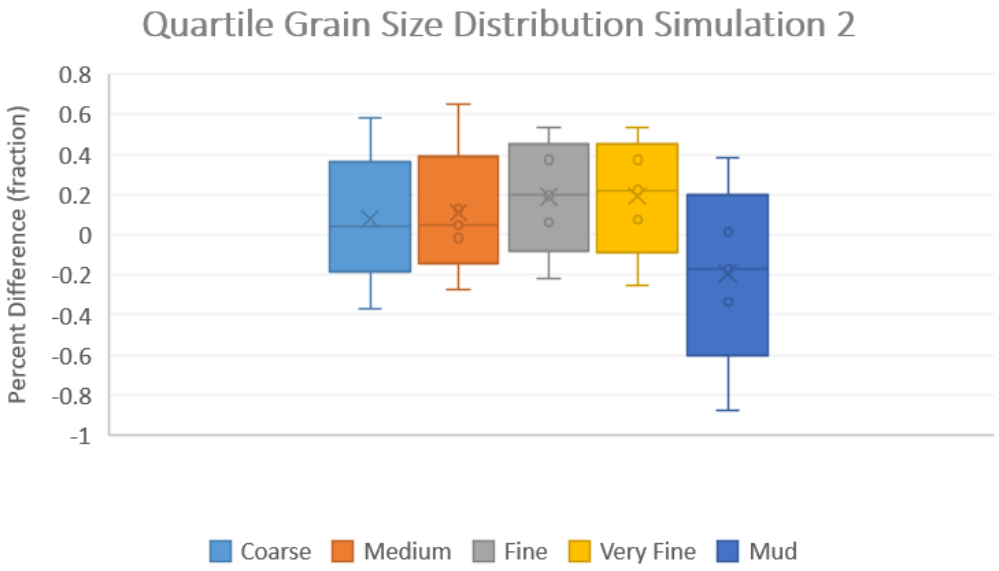

Figure 29: Quartile grain size distribution for the five grain size classes for Simulation 2. "X" indicates mean value.

The results of Simulation 2 show an overall similarity to Simulation 1 with coarse and medium containing the lowest average difference, and fine and very fine containing a higher average difference. Overall, the average percent difference is higher for each of the five grain size classes, including mud. Once again, the coarse and medium grained sediments contain the lower average, but a higher spread when compared to the fine and very fine grained material. The size and shape of the sand lobe is almost identical to that of Simulation 1. The prodelta that is deposited is larger than that of Simulation 1, extending approximately a half a kilometer farther into the basin. Even with the additional mud within the system, there is a noticeable lack of prodelta directly in front of the sand lobe.

5.2.5 Simulation 3

Table 9: Average percent difference between the interpolation data and the simulation results for each grain size class from Simulation 3. Negative values indicate higher percentages in the simulations.

	Coarse	Medium	Fine	Very Fine	Mud
Average	4%	4%	18%	19%	-12%

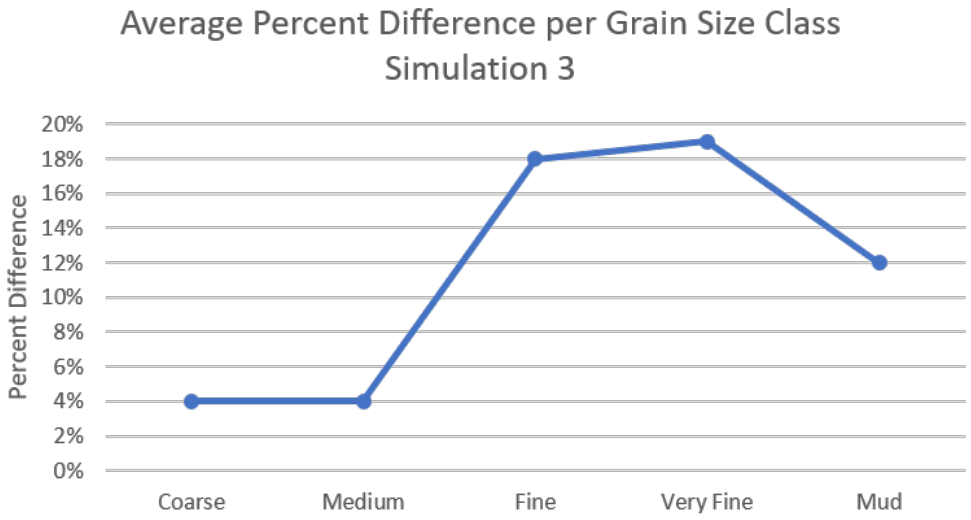

Figure 30: Average percent difference between interpolation and model results for each grain size class in Simulation 3.

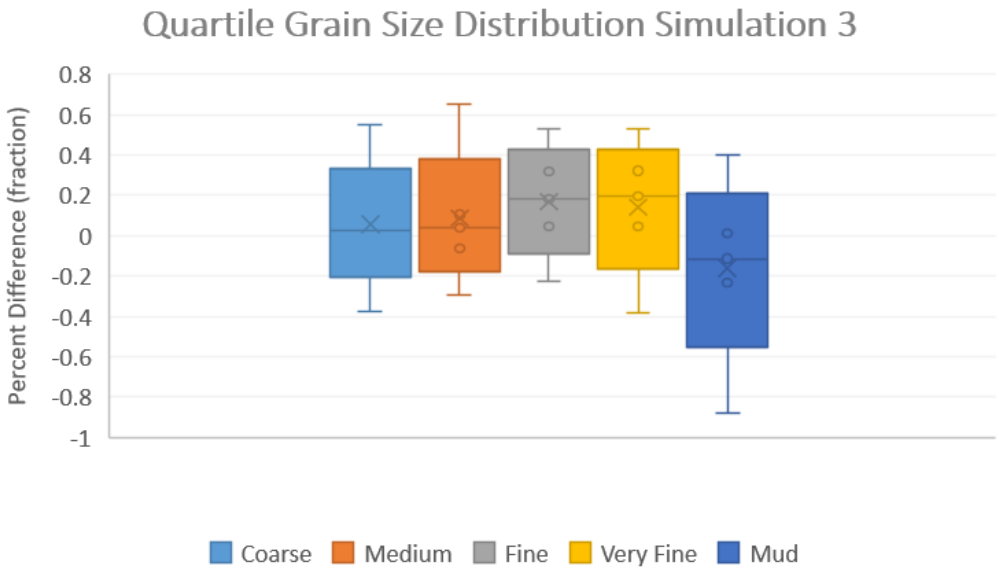

Figure 31: Quartile grain size distribution for the five grain size classes for Simulation 3. "X" indicates mean value.

The results of Simulation 3 are more comparable to Simulation 1 than to Simulation 2. The removal of the calcite within the system resulted in the lowest average percent difference for the four sand classes, and a slight

increase for the mud class. An average percent difference of 4% is present for the coarse and medium grain size classes. Fine has an average difference of 18% and very fine has an average difference of 19%. The difference between the two data sets for mud increases 2% to 12%. The shape of the lobe is very similar to that of Simulation 1. The largest difference being the lateral width of the lobe at the farthest point into the basin. Simulation 3 contains a much wider distal section of the lobe than compared to that of Simulation 1. Simulation 1 contains two main channels that feed sediment into the basin, while Simulation 3 contains a series of smaller channels that transport sediment to different sections of the lobe, as opposed to just the central edge of the lobe.

5.2.6 Simulation 4

Table 10: Average percent difference between the interpolation data and the simulation results for each grain size class from Simulation 3. Negative values indicate higher percentages in the simulations.

	Coarse	Medium	Fine	Very Fine	Mud
Average	8%	8%	22%	23%	-13%

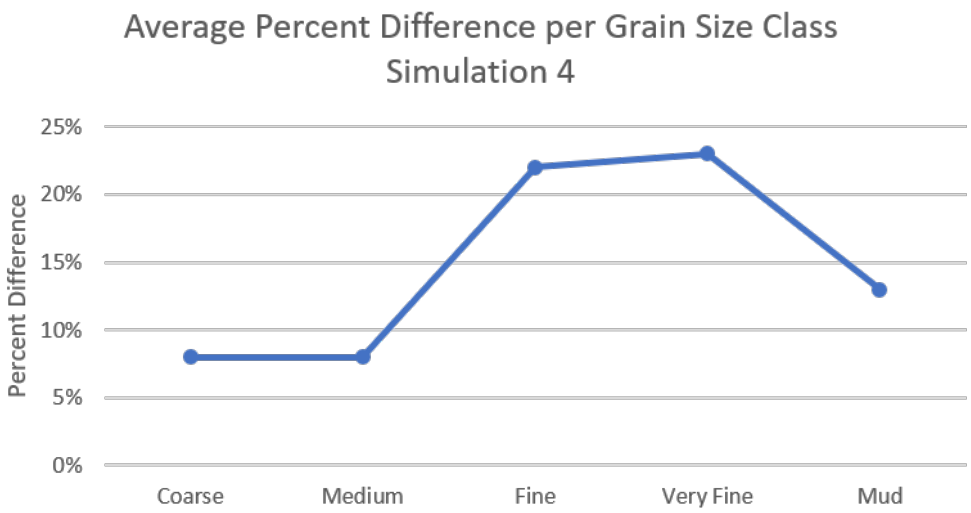

Figure 32: Average percent difference between interpolation and model results for each grain size class in Simulation 3.

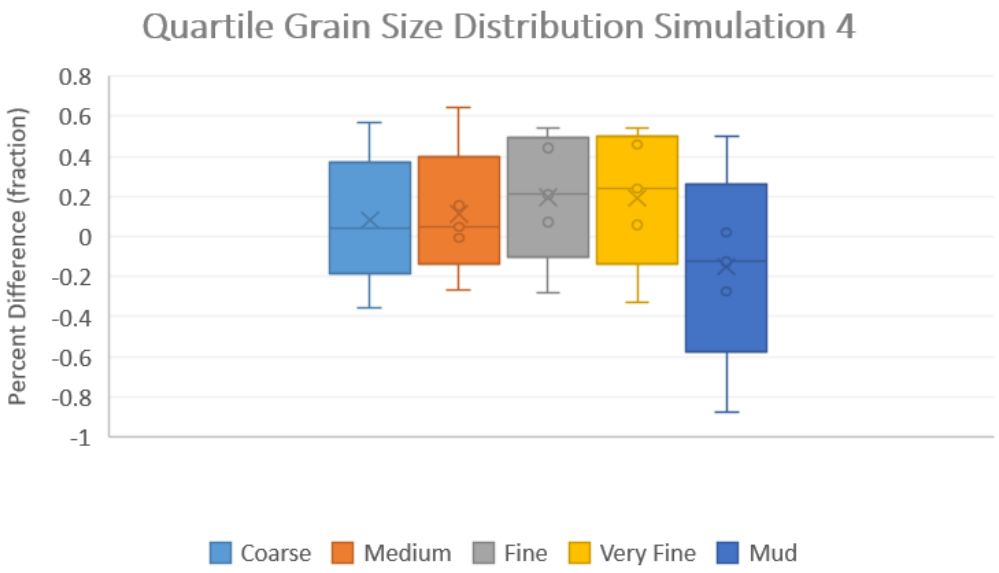

Figure 33: Quartile grain size distribution for the five grain size classes for Simulation 3. "X" indicates mean value.

Simulation 4 altered the critical bed shear stress for erosion within the system. As shown above in Figure 24, the resulting shape is drastically different than the other simulations. The sand lobe displays an elongated shape, extending approximately a kilometers farther into the basin when compared to Simulation 1. Along the eastern edge of the sand lobe, a small prodelta is present. On the west side of the sand lobe, a prodelta is not found. A single large channel is present that runs from the river mouth towards the basin. The difference between the two data sets increases for each of the grain size classes. Coarse and medium grains are up to 8% difference. Fine and very fine increase to 22% and 23%, with mud increases 3% to 13% when compared to Simulation 1.

5.2.7 Simulation 5

Table 11: Average percent difference between the interpolation data and the simulation results for each grain size class from Simulation 3. Negative values indicate higher percentages in the simulations.

	Coarse	Medium	Fine	Very Fine	Mud
Average	5%	5%	17%	18%	-10%

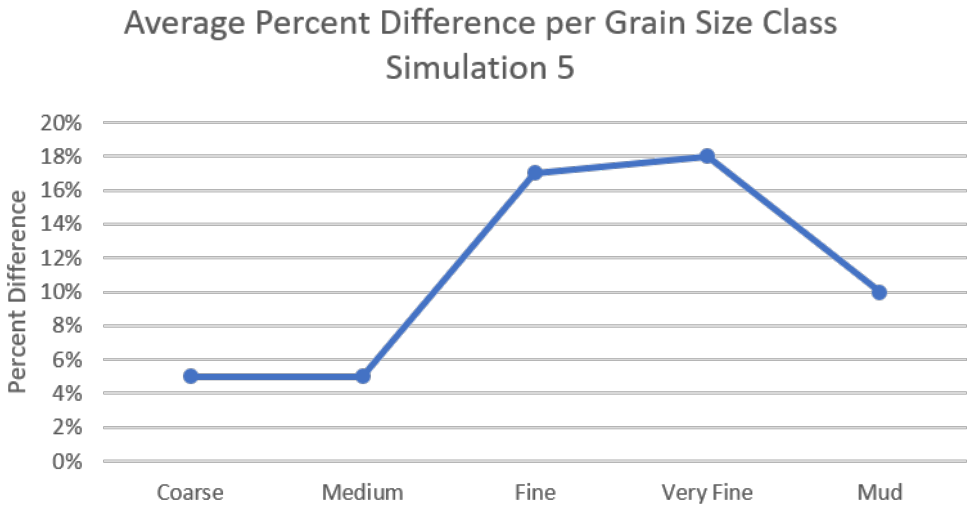

Figure 34: Average percent difference between interpolation and model results for each grain size class in Simulation 5.

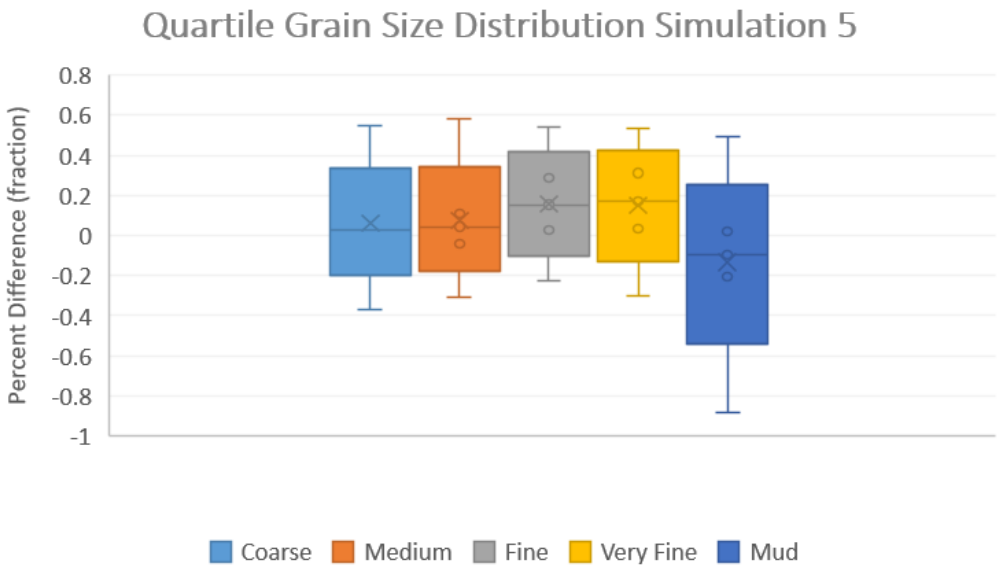

Figure 35: Quartile grain size distribution for the five grain size classes for Simulation 5. "X" indicates mean value.

Simulation 5 reduced the concentration of mud during deposition. The results show an average difference of 5% for both the coarse and medium sized grains, identical to Simulation 1. Fine grains contain a 17% difference, and very fine displaying a 18% difference between the two data sets. Mud contains a 10% difference, the same as Simulation 1. The shape of the sand lobe generated is similar to that of Simulation 1, with the lobe being larger laterally at the most distal point within the basin. The prodelta that is deposited does not extend into the basin as far when compared to Simulation 1.

5.2.8 Average Grain Size Per Sample Location

Within each of the five models, nine locations were chosen within the generated sand lobe that represent the locations from which the field samples were collected. The mean grain size was then calculated for each sample location. The results were then compared to the mean grain size of the samples collected from the field. Sample Y18 did not fall within the sand lobe in the simulations, as a result it was not included in this analysis.

Table 12: Mean grain size for 8 sample locations within the sand lobe from all five simulations and the corresponding field location.

	Mean Grain Size (mm)					
Sample	Simulation 1	Simulation 2	Simulation 3	Simulation 4	Simulation 5	Field Data
Y2	253	191	228	133	197	112
Y3	161	193	257	148	217	116
Y9	152	206	239	196	215	260
Y14A	205	183	202	204	198	385
Y15	202	198	210	263	191	374
Y16	206	178	207	174	179	276
Y19	204	158	191	131	190	118
ZY	132	177	172	167	150	540

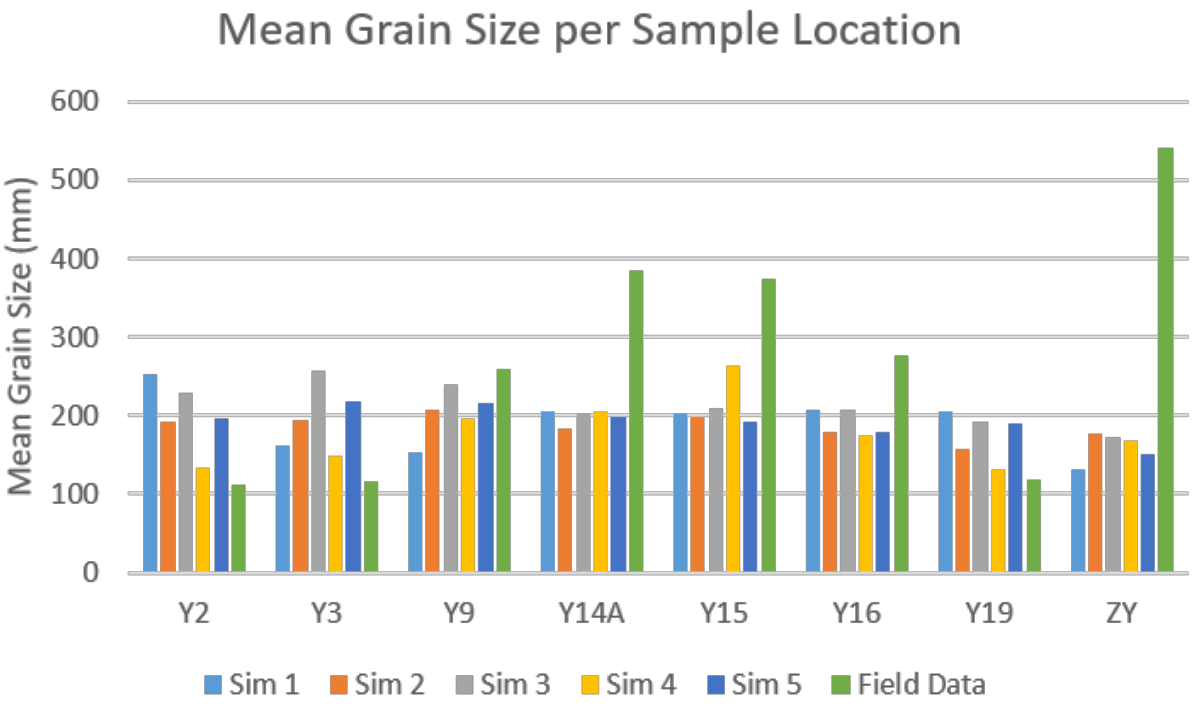

Figure 36: Mean grain size (mm) of each of the sample locations within the simulations, as well as the field data.

5.3 Discussion

With the results from each of the simulations, it was possible to analyze how each of the studied input parameters affected the final results of the simulations, as well as further analyze the results of the best calibrated model. This will provide insight on which parameters have the highest affect on the overall system.

5.3.1 Simulation 1

The first simulation involved using the grain size concentrations observed from the thin section analysis, as well as an increased mud concentration of 0.05 kg/m^3. This simulation was viewed as the baseline of all the other simulations, as the parameters were observed from the outcrop data, excluding mud. While the mud concentration was modified, it was done so to the best estimate of what was actually present during deposition.

While the prodelta is deposited extensively on the laterally distal sections of the lobe, it was not deposited in front of the central section of the lobe. This is caused by the waves and tide pushing the suspended mud back towards the shoreline along the edges of the lobe where it is then deposited. Channels can be observed that run from the river mouth out to the distal edge of the sand lobe. Smaller channels are observed that deliver sediment towards the lateral edges of the lobe. The final shape of the sand lobe can be found in Figure 25 above.

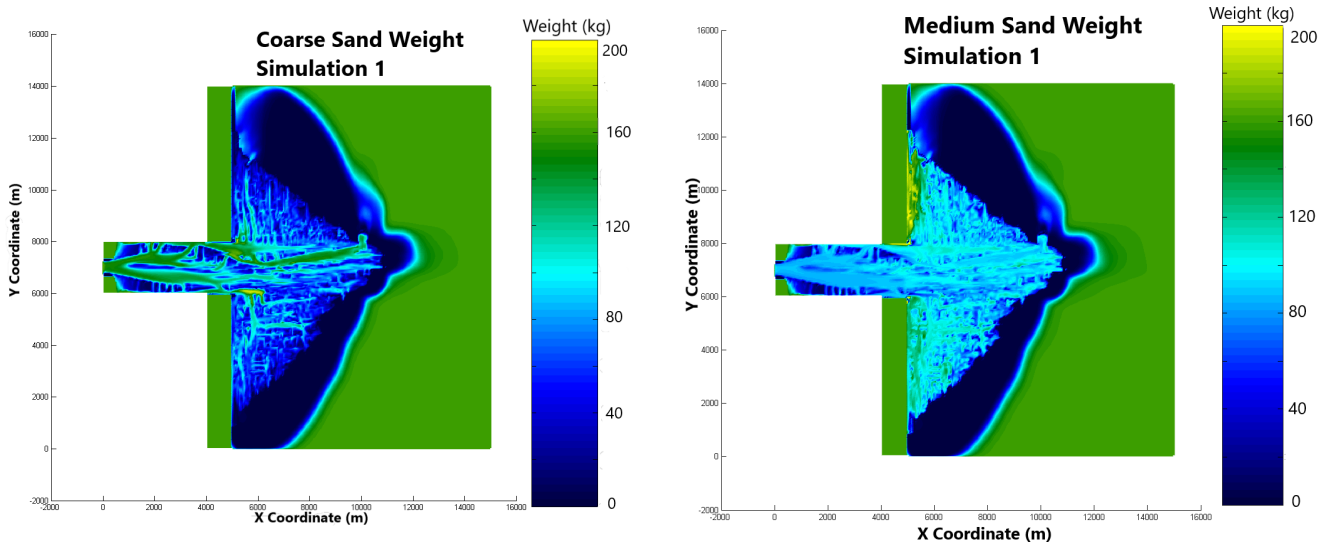

Figure 37: Weight of coarse and medium grained sand deposited throughout the sand lobe for Simulation 1.

Figure 37 above displays the weight of coarse and medium sized grains. Coarse grains tend to be deposited along the central channels that run towards the edge of the lobe directly from the river mouth. When looking at the distribution of the medium sized grains, larger amounts of sediment is deposited along the smaller channels that run parallel to the coastline. Once these smaller channels branch off the main central channel, they do not contain enough energy to carry the coarse sized grains. As a result, the medium grained sand is deposited over the entire sand lobe and the coarse grained material is isolated to the central area of the lobe, which is what is observed in the field.

The results of the simulation show a high correlation in the data from the interpolation for medium and coarse grained material. The difference between the two data sets is 5% for coarse sand and 5% for medium sand over the entire lobe, with the interpolations containing higher concentrations of coarse and medium sediment. This indicates a high correlation between the model and the field data. As you move into the more distal sections, the correlation becomes less. For fine grained sand, a difference of 20% is observed and 21% for very fine sand. It is apparent that the difference between the interpolated data and the simulation becomes more drastic as you move into finer grained sediments. When comparing the depositional trends for each of the grain size classes, it was observed that for all the grain size classes, excluding mud, a higher average concentration was present within the interpolated data than compared to the simulation results. For mud, the simulation produces more mud throughout the entire system than what is observed in the interpolated data.

5.3.2 Simulation 2

Simulation 2 differs from the first simulation in that the concentration of mud was increased from 0.050 kg/m^3 to 0.080 kg/m^3. The mud concentration was increased to see how it affects the overall system, as it is difficult to gauge the amount of sediment present during transport and deposition as the large majority is eroded and washed away.

With the additional mud in the system, the percent difference between the interpolation data and the model results slightly increased throughout the entire lobe. In regards to the coarser material, the percent different for coarse is 7%, up from 5% in Simulation 1. For medium sized grains, the difference increased as well, up from 5% in Simulation 1 to 7% in Simulation 2. While the results for coarse and medium sized grains for Simulation 2 are still favorable, they contain a larger average difference than Simulation 1. For fine grained material, Simulation 2 produced an average difference of 21%, an increase of only 1% from Simulation 1. A 1% increase in difference was observed as well for very fine grains in Simulation 2, up now to 22%. The average difference for mud increased as well, now to -18%.

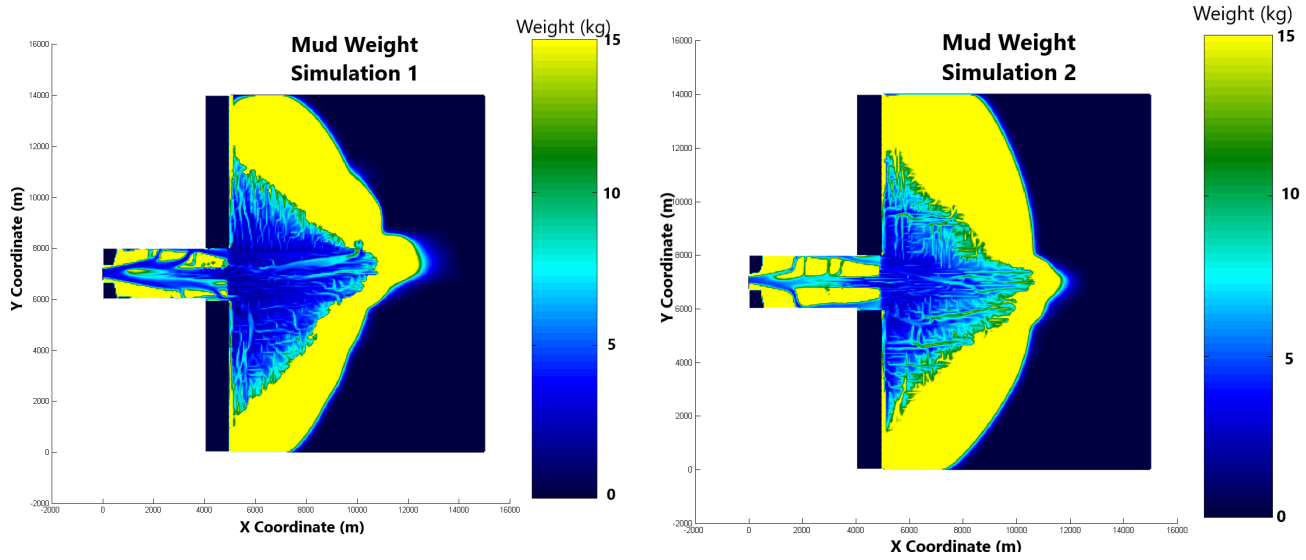

Figure 38: Weight of mud deposited within the system for Simulations 1 and 2. The scale has been lowered to increase the visibility of values within the lobe.

As shown above in Figure 38, there is considerably more mud deposited within the sand lobe in Simulation 2 as composed to Simulation 1. Within Simulation 1, mud deposited within the sand lobe is confined to the outer edges and within channels at the boundary of the lobe. In Simulation 2, mud is deposited in more central locations, as well in higher concentrations compared to Simulation 1. This leads to higher mud percentages and an increase in difference between the interpolation data and model results.

The simulation produces a low variation in grain size distribution between the two data sets for coarse and medium sized grains. Fine and very fined grains increased marginally when compared to Simulation 1, but still contain a high average contrast to the interpolation data. With high amounts of mud being added to the system, the already high difference in mud percentage increased to now close to -18%.

5.3.3 Simulation 3

Simulation 3 measured the affect that carbonate has on the system. In previous simulations, very fine grained sediment was split into two categories, one with a density of sand, and another with the density of carbonate. In this simulation, the carbonate density was removed, resulting in the same total concentration, but now a single density for the grain size class.

For coarse grains, a difference of only 4% is observed between the interpolated data and the model simulations, down from 5% in Simulation 1. For medium sized grains, the average difference decreased from 5% in Simulation 1, to 4% in Simulation 3. Fine grained sand has an average difference of 18% and very fine sand has a difference of 19%. The average difference for both fine and very fine sand decreased when compared to Simulation 1. For mud, an average of -12% is observed, a 2% decrease in accuracy when compared to Simulation 1.

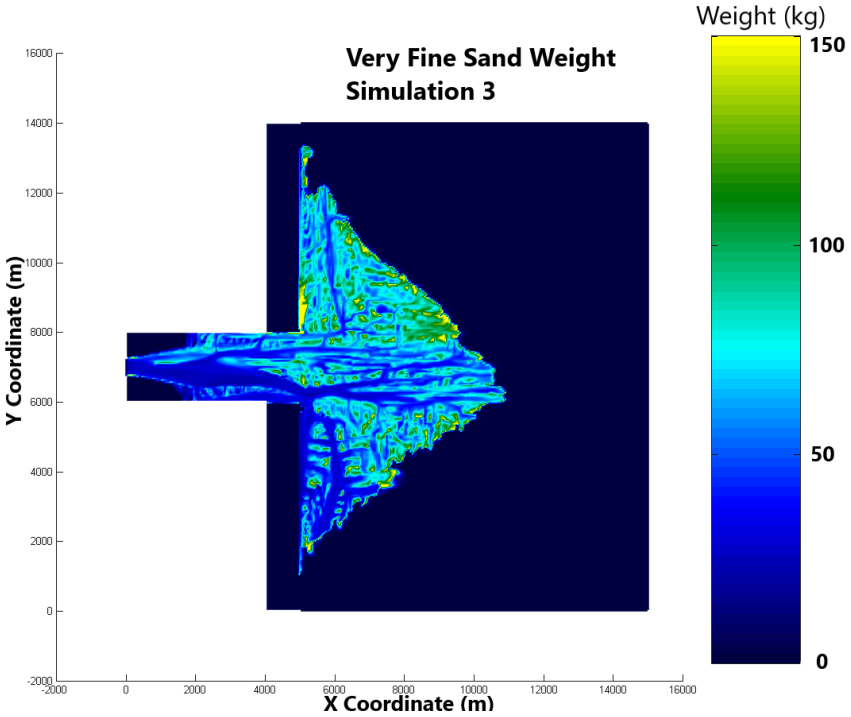

Figure 39: Weight of very fine sediment deposited in Simulation 3. Scale has been lowered to increased visibility of values within the sand lobe.

The depositional trends for very fine grained sand is shown above in Figure 39. The majority of the very fine grained sediments were deposited along the outer boundary of the lobe, while smaller amounts were deposited in between the channel network of the lobe. In locations where zero deposition occurred, they can be directly linked to the locations of channels, as the energy involved in these areas is too high for the sediment to be deposited. Very fine grains can be found in the proximal setting directly in front of the river mouth, which are not found in the interpolation data. This is one of the factors that lead to a relatively high difference between the interpolation and simulation data.

For every grain size class, the average difference between the interpolated data and the simulation results was lower than that of Simulation 1 and 2. This indicates that the densities present for each of the grain size classes play a large role in the grain size distribution for the sand lobe.

5.3.4 Simulation 4

Simulation 4 tested the effects that erosion has on the system. The critical bed shear stress for erosion (TcEro) in cohesive sediment was increased from 0.12 N/m^2 to 0.3 N/m^2. Increasing the TcEro requires higher amounts of energy for erosion to take place.

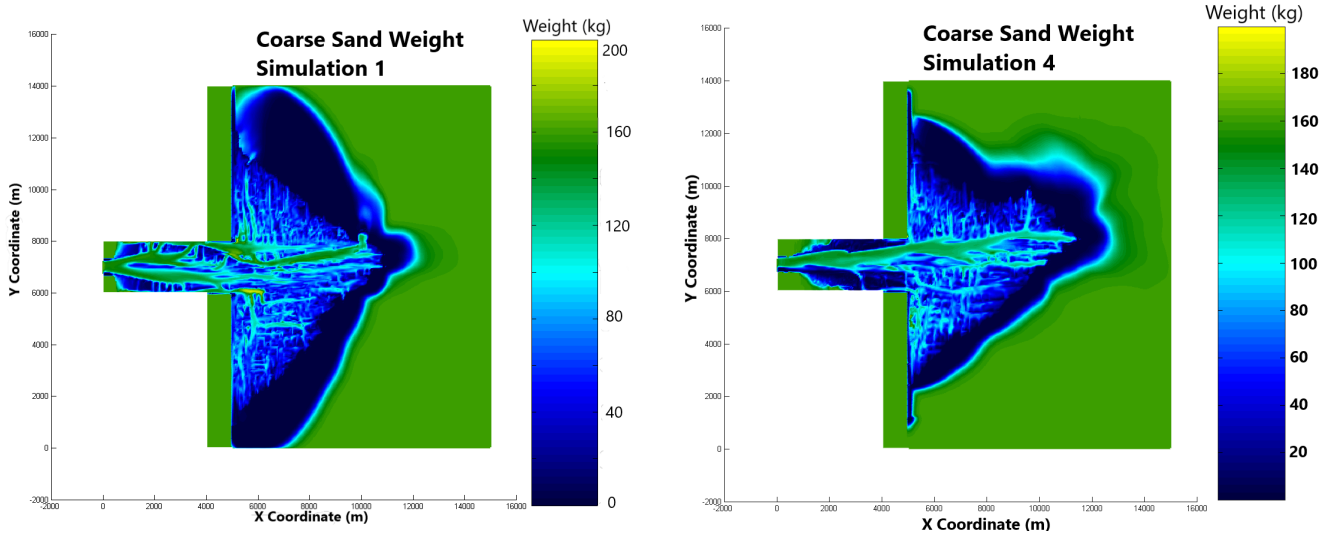

Figure 40: Weight of coarse sand deposited within the system for Simulations 1 and 4.

As shown in the figure above, the shape of the sand lobe of simulation 4 is substantially different to that of Simulation 1. In the early stages of the sand lobe, a mud deposit is deposited initially over the area in front of the river mouth. With the change to the amount of energy required for erosion, the amount of channels formed decreased. In Simulation 1, a large channel network is present that transports sediment towards the later sections of the sand lobe. In Simulation 4, the channel network is much smaller and does not extend as far into the lateral sections. The loss of energy outside the main central channel is large, therefore it is not possible to erode new channels. As a result, the majority of sediment is deposited in the proximity of the main central channel.

The average difference for coarse grains increases by 3% when compared to Simulation 1, up from 5% to 8%. The same trend is observed for the medium grain size distribution, increasing 3% to 8%. The change for fine and very fine grains is smaller, but still increases when compared to Simulation 1. The difference for fine grains is 22%, up from 20%. Very fine grained sediment increases 2% to 23%. Mud increases 3% to -13%. It is apparent that increasing the TcEro has drastic affects on the system. In this simulation, every grain size class saw large increases in the difference between the interpolated data and the simulation results.

5.3.5 Simulation 5

The final simulation that was run involved using the mud concentration that was observed from the thin section and interpolation analysis. The mud concentration was dropped from 0.05 kg/m^3 in Simulation 1, to 0.0147 kg/m^3. The resulting sand lobe maintained a similar overall shape to that of Simulation 1, with a less extensive prodelta. Once again, the prodelta is more extensive along the eastern edge of the boundary.

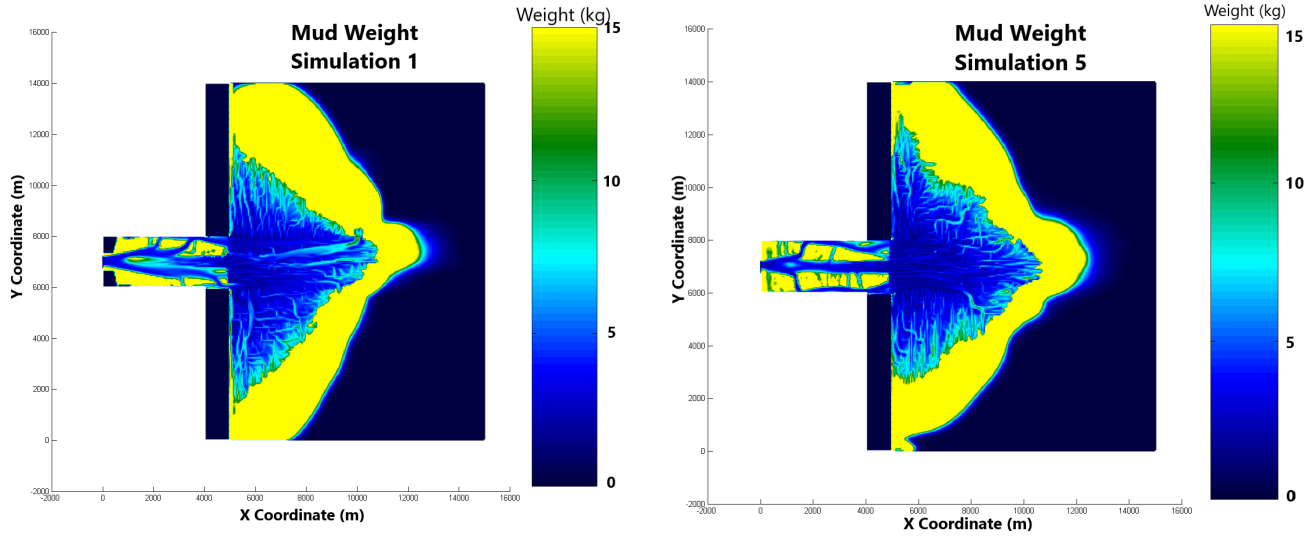

Figure 41: Weight of mud deposited within the system for Simulation 1 and 5. The scale has been lowered to increase the visibility of values within the lobe.

The difference in grain size distribution for both coarse and medium sized grains is comparable to that of Simulation 1. Coarse and medium sized grains both contain an average difference of 5%. The difference for fine grained sand decreased 3% to 17%. For the very fine grained sediment class, Simulation 5 was 3% lower than Simulation 1, with a value of 18%. The percent difference for mud is -10%, identical to that of Simulation 1. The effects of lowering the mud concentration input value were most seen in the grain size distribution for the fine and very fine grain size classes.

5.3.6 Model with Highest Calibration

With each of the Simulation results analyzed, the model with the highest calibration was chosen. The model was chosen based off the average percent difference for each of the grain size classes, overall shape of the sand lobe, and the impact the varied input value had on the entire system.

When analyzing the average percent difference between the interpolated data and the simulated data, Simulation 3 and 5 contain much lower average differences for each of the grain size classes when compared to the remaining 3 simulations. Simulation 3 displays a higher calibration for coarse and medium sand, with Simulation 5 having a higher calibration for very fine, fine, and mud sediment. With Simulation 3 not incorporating carbonate in the system, Simulation 5 is chosen as the model with the highest calibration.

When analyzing the difference in mean grain size for each sample location, as shown in Table 12, we can compare the results of the simulation with the data collected from the field at each sample location. This will indicate the calibration at the location of each of the samples. In the proximal setting, sample Y2 has a mean grain size that falls within the "fine" grained category for both the simulation data and the field data. Within the central location of the lobe, the four samples, Y14A, Y15, Y16, and ZY, display varying results. Within the simulation data, the mean grain size ranges from 150 mm to 198 mm, all within the "fine" grain size class. The field data ranges from a minimum of 175 mm, up to 303 mm for sample ZY. This results in samples Y15

and Y16 being in the "fine" grained category, while samples Y14A and ZY are within the "medium" class. For samples Y15 and Y16, the difference between the field data and the simulation data is low, 5% for Y15, and 3% for Y16. In the distal locations, the simulation data contained a coarser mean grain size aver than compared to the field data. The field data, with the exception of sample Y9, were all within the "very fine" category, while all of the simulation results were within the "fine" grained category. The largest difference was observed in the location of sample Y19, with a mean average grain size of 190 mm for the simulation, and 89 mm for the field data.

The average percent difference between Simulation 5 and the interpolated data set was discussed above, this section will discuss which locations in the sand lobe contain a high calibration, and those which poorly represent the real-world data. The percent difference between the interpolated data and the model results was plotted to display an overview of the calibration in different sections of the lobe. While the simulation generated a sand lobe larger than the area of the grain size interpolation, only the area equivalent to the interpolation will be plotted, as these are the only locations in which points from both data sets are present. The results are shown below in Figure 42.

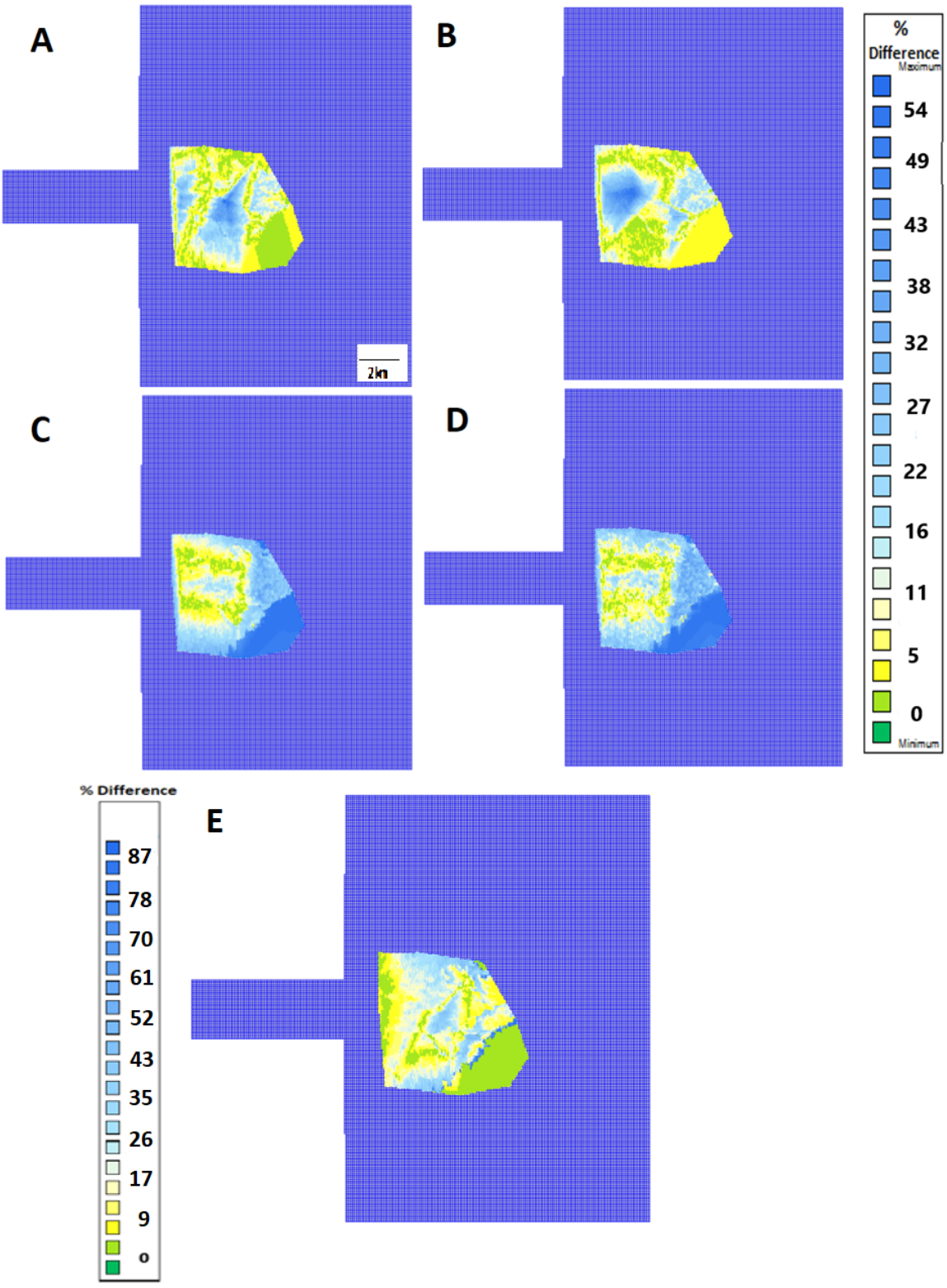

Figure 42: Percent difference between the grain size interpolation and the model results at each individual location for the five grain size classes, (A) Coarse, (B) Medium, (C) Fine, (D) Very Fine, (E) Mud. The mud distribution contains a unique legend that is only applicable to this grain size class. Low percentages indicate a small difference between the two data sets.

When analyzing the results in Figure 42, different grain size distribution trends become apparent. The most noticeable aspect for each of the grain size classes is the bottom right section of the sand lobe. For coarse and

medium grained sediments, this is a location of little variation between the two data sets, but for the remaining grain size classes, this represents a large discrepancy between the two. This is caused by the difference in shape between the interpolated sand lobe and the model results. Within the simulations, this location is part of the delta front, composed of predominately mud, while it is considered part of the sand lobe in the interpolation data. This results in very large differences between the two data sets for the fine, very fine, and mud grain size classes. As a result, this brings the average percent difference between the interpolation data and the simulation data up to a much higher value. Values with a mud percent greater than 90% were removed, as they are representative of prodelta deposits.

When analyzing the fine and very fine distribution, both grain size classes display a high correlation between the two data sets. In the proximal locations, the average percent difference ranges between 0-10%. As you move to the outer sections of the lobe, the difference increases to an average of 16-22%. Once again, the section representing the delta front in the simulations contains the highest percent difference, up to 54%. When analyzing the distribution for coarse and medium sized grains, the results tend to be random in nature. For coarse grains, large percent differences are observed within the middle of the sand lobe. In the interpolated data, this location is predominately coarse grained. Within the simulations, the coarse material was only deposited within the channels that were created within the lobe. As a result, the coarse sand did not cover all parts of the lobe, leading to higher differences between the two data sets. For medium grained sand, the area directly in front of the river mouth contains a large difference between the interpolation and simulation results. The interpolation data contains large percentages of medium grained sand, up to 54%, directly in front of the river mouth. While the simulation deposits medium grained sediment in these locations, it is not in the high amount found in the interpolation data.

Sample Y18 was collected at the edge of the sand lobe, representative of the most distal environment, while still located within the sand lobe. The location of this sample within the interpolation data ended up outside of the simulation area, but its representative depositional environment within the lobe can be analyzed. Within the generated sand lobe, a location along the distal edge of the sand lobe was selected that is representative of where sample Y18 was collected within the Roda Y. The location of the point selected is shown below in Figure 43. The mean grain size was calculated using the same technique in Figure 36, and the results were compared to the mean grain size of the field data. The field data has a mean grain size of 126 mm and the simulation data has a mean grain size of 119 mm. The difference between these two values is only 6%. This shows that while some values contain relatively high differences between the data sets when comparing the same location, the similar depositional environments contain a high correlation between the outcrop data and the simulation results.

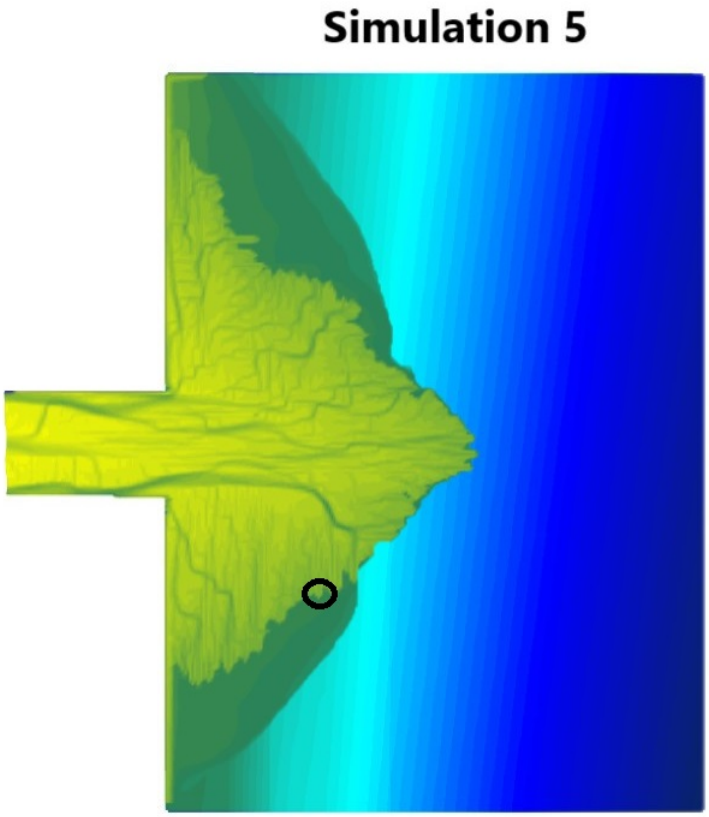

Figure 43: Location of additional sample represented by a black circle.

When analyzing the mean grain size values in Figure 36, samples Y14A, Y15, and ZY contain a large difference in the results of Simulation 5 and the field data. The field data contains a much higher mean grain size than the simulation results. When analyzing the sediment distribution in the models, it is apparent that the coarsest materials are found within the main channel that is running perpendicular to the shoreline. The location of the data points from which the simulation data was collected lies outside of these channels. If a location within the coarse channel is tested, a mean grain size value of 260 mm. When comparing this value with samples Y14A and Y15, which have mean grain size values of 385 mm and 374 mm, the difference drops drastically. The simulation result and the field data are both representative of the medium grain size class. This compliments the findings in the paragraph above regarding Sample Y18 in that when sampling the relative depositional environment within the sand lobe, the correlation is high. Comparing the exact sample locations provides a good rough estimate of the correlation through the general area, but it is not as beneficial as comparing the relative depositional environments.

Through the detailed analysis of Simulation 5, as well as the other simulations, we were able to come to a conclusion about the degree of calibration for the model. For coarse and medium grained sand, the calibration is very favorable, displaying only small variances from the real world data. For the remaining grain sizes, the calibration is less optimal. The main issue involved in the calibration is the difference in the size and shape of the sand lobe when comparing the interpolated data and the results of the simulation. When performing the interpolation, the size and shape of the lobe is estimated based off of information gathered from the field,

as well as literature. In this case, the simulation produced a sand lobe that was larger than the interpolated lobe, as well as a different shape. This results in some of the field data points being located in different sections of the sand lobe in the two scenarios. For example, sample Y18 is at the very edge of the sand lobe in the interpolation data, but is found within the prodelta in the simulations. As a result, it can depict a very different grain size distribution trend. This explains the large differences found for the fine, very fine, and mud grain size classes. As mentioned above, when analyzing specific depositional environments within the lobe, such as the location of sample Y18, a high correlation is present. This indicates that when the size and shape are representative of the real world data, the resulting grain size distribution shows a high calibration to the real world data.

The resulting shape of the sand lobes generated within the simulations did not ideally match the shape of a Gilbert-type sand lobe. This issue is the main focus for further testing. Further tests of additional parameters, as well as possible modifications to the bathymetry of the basin, could be the way to achieve a more favorable sand lobe geometry. These were not tested due to time constraints involved with simulation times. This thesis has shown that in locations in which the two sand lobes contain similar depositional locations within the sand lobe, a high calibration is present. These results indicate that a simulated sand lobe similar in size and shape to the interpolated data set will produce a model with a high calibration throughout.

6 Conclusion and Recommendations

The use of process-based modelling within the oil and gas industry is still very new, and has the ability to become one of the tools in the future that companies use to solve issues involved in reservoir modelling. This thesis involved the initial steps required to test the viability of using process-based models to better model heterogeneities within the reservoir. The Gilbert-type deltaic deposits of the Roda Y Sandstone in Northern Spain provided a great opportunity to test the calibration potential of process-based models.

The Roda Y Sandstone contains a variety of grain size distributions based on the location within the sand lobe. Nine samples were collected throughout the sand lobe and analyzed to obtain the grain size distribution throughout the fan delta. The proximal setting of the lobe contains a combination of fine and medium grained sediments. Within the central locations of the sand lobe, high concentrations of coarse and medium grains are found. Along the distal boundaries of the lobe, the grain size distribution is predominately fine and very fined grained. Small amounts of mud are found throughout the system as well.

Each of the five simulations produced unique results based off the input parameter that was varied. The shape and size of the resulting sand lobes were comparable, with the exception of Simulation 4, where the critical shear stress for erosion was modified. The grain size distribution followed very similar trends throughout all the simulations, with each simulation varying slightly from the last. The grain size distribution of the simulations were then compared to that of the field interpolated data set. Coarse and medium sized grains exhibit a high match throughout the lobe, while fine and very fine grains contain a higher percent difference between the two data sets.

Simulation 5 was chosen as the model that is the closest representation to that of the field interpolation data. The difference between the two data sets for coarse and medium grains is only 5%, while the average percent difference for fine grains is 17% and 18% for very fine. Mud has an average difference of -10%. The mud deposited within the lobe in Simulation 5 is restricted to the outer edges of the sand lobe, which is representative of what is found in the field. For all grain sizes excluding mud, the grain size interpolation contained a higher average concentration for each grain size class.

The issues and errors involved in this process are centered around the shape of the lobe that is being created. When interpolating the field data, an overall shape for the sand lobe is estimated. The larger the difference in shape between the the interpolated data and the simulation lobe, the larger the difference in the results. This is visible in the results for fine and very fine grained sediments, as the percent difference between the two data sets is much higher than the coarse and medium sized grains, which are found in more proximal settings.

With the shape of the sand lobe not precisely matching the shape observed in the field, the results at specific locations must be noted as they are not always within the same depositional location. To account for this, measurements were taken at locations within the sand lobe that represent where the field samples were

collected. The correlation between these comparisons is high, indicating that simulations are highly calibrated throughout the different sections of the sand lobe.

Future work would involve addressing the issue regarding the shape of the sand lobe. This involves further studying of additional parameters and how they affect the results. With the large amount of parameters present within Delft3d, continual testing is needed to find the ideal combination of modified parameters to produce the ideal sand lobe shape. Additional interpolation methods for the field data can be tested as well. This thesis utilized only one interpolation method, but other methods can be tested to achieve the most favorable results. To further study the calibration of the simulated model, additional grain size studies on the outcrop would be beneficial, specifically measuring the change in grain size over small distances. As Gilbert-type deltas typically display coarsening upward trends, the vertical change in grain size at each sample location can be measured and compared to that of the simulation. This will require an extensive sedimentological study of the outcrop. This is particular difficult due to the lack of field data that is present. Large sections of Roda outcrops are difficult to access and therefore the locations in which samples can be taken is limited.

As this thesis was just the initial step of an overall topic, the next step would involve beginning to model the heterogeneities within the lobe. The main obstacle to overcome with this process is the scale of the grid. As the majority of the heterogeneities found within the sand lobe are less than 10 meters in size, and the grid having dimensions of 50 meters by 50 meters, a solution will have to be constructed to overcome this scaling issue.

7 References

Clemetsen, R., Hurst, A., Knarud, R., & Omre, K. H. (1990). A Computer Program for Evaulation of Fluvial Reservoirs. 373-385.

Coll, M., López-Blanco, M., Queralt, P., Ledo, J., & Marcuello, A. (2013). Architectural characterization of a delta-front reservoir analogue combining Ground Penetrating Radar and Electrical Resistivity Tomography: Roda Sandstone (Lower Eocene, Gaus-Tremp basin, Spain). *Geologica Acta, Vol. 11*, 27-43.

Crumeyrolle, P., Lesueur , J., Claude, D., & Joseph , P. (1992). Architecture et facies d'un prisme deltaique de bas niveau marin: les gres de Roda (bassin eocene sud Pyreneen.). *Livret-guide de l'excursion ASF*, (p. 36). Paris.

Faculty and Institute of Actuaries. (1997). Description of Stochastic Models. *Claims Reserving Manual*.

Ferrer-Boix, C., Martin-Vide, J. P., & Parker, G. (2015). Sorting of a sand-gravel mixture in a Gilbert-type delta. *Sedimentology*, 1446-1465.

Gobo, K. (2014). *Development of Gilbert-type deltas: sedimentological case studies from the Plio-Pleistocene of Corinth Rift, Greece.* Bergen.

Hubbard, S. M., Covault, J. A., Fildani, A., & Romans, B. W. (2014). Sediment transfer and deposition in slope channels: Deciphering the record of enigmatic deep-sea processes from outcrop. *GSA Bulletin*, 857-871.

Joseph, P., Hu, L. Y., Dubrule, O., Claude, D., Crumeyrolle, P., Lesueur, J. L., & Soudet, H. J. (1993). The Roda Deltaic Complex (Spain): From Sedimentology to Reservoir Stochastic Modelling. *Subsurface Reservoir Characterization from Outcrop Obsercations*, 97-109.

Karssenberg, D., Törnqvist, T. E., & Bridge, J. S. (2000). *Conditioning a Process-Based Model of Sedimentary Architecture to Well Data.*

Koltermann, C. E., & Gorelick, S. M. (1996). Heterogeneity in sedimentary deposits: A review of structure-imitating, process-imitating, and descriptive approaches. *Water Resources Research*, 2617-2658.

Leren, B. L., Howell, J., Enge, H., & Martinius, A. (2010). Controls on stratigraphic architecture in contemporaneous delta systems from the Eocene Roda Sandstone, Tremp-Graus Basin, northern Spain. *Sedimentary Geology* , 9-40.

López-Blanco, M., Marzo, M., & Muñoz, J. (2003). Low-amplitude, synsedimentary folding of a deltaic complex: Roda Sandstone (lower Eocene), South-Pyrenean Foreland Basin. *Basin Research*, 73-95.

Martinius, A. W. (2012). Contrasting Styles of Siliciclastic Tidal Deposits in a Developing Thrust-Sheet-Top Basins - The Lower Eoce e of the Central Pyrenees (Spain). *Principles of Tidal Sedimentology*, 473-506.

Martinius, A. W. (2017). Multiscale Gilbert-type delta lobe architecture and heterogeneities: The case of the Roda Sandstone Member. *AAPG Bulletin, V. 101, No. 4*, 453-463.

Michaud, K. J. (2011). *Facies Architecture and Stratigraphy of Tidal Ridges in the Eocene Formation, Northern Spain.* Ontario.

Michaud, K. J. (n.d.). *Facies Architecture and Stratigraphy of Tidal Ridges in the Eocene Roda Formation, Northern Spain.*

Milliman, J., & Farnsworth, K. (2011). *River Discharge to the Coastal Ocean - A Global Synthesis.* Cambridge University Press.

Molenaar, N. (1990). Calcite Cementation in Shallow Marine Eocene Sandstones and Constraints of Early Diagenesis. *Journal of hte Geological Society*.

Mullins, J. R., Howell, J., van der Vegt, H., Buckley, S., & Storms, J. (2017). Evaluation the Appliation of Process-Based Models as Training Images for Multiple Point Statistics. *AAPG Annual Convention and Exhibition.* Houston.

Nijman, W., & Nio, S. (1975). The Eocene Montanana Delta (Tremp-Graus Basin, provinces of LErida and Huesca, South Pyrenees, Spain). *The Sdeimentary Evolution of the Paleogene South-Pyrenean Basin*, 1-20.

Nio, S. D., & Yang, C. S. (1991). Sea-level fluctuations and the geometric variability of tide-dominated sandbodies. *Sedimentary Geology*, 161-193.

Nio, S., Siengenthaler, C., & Yang, C. (1984). Facies Pattern and Development of the Lower Eocene Roda Sandstone, Isabena Valley, Southern Pyrenees, Spain. *IAS European Regional Meeting*, 328-239.

Postma, G. (2003). Fan Delta. In G. V. Middleton, *Encyclopedia of Sediments and Sedimentary Rocks* (pp. 272-274). Boston: Kluwer Academic Publishers.

Puigdefàbregas, C., Muñoz, J., & Vergés, J. (1992). Thrusting and foreland basin evolution in the Southern Pyrenees. *Thrust Tectonics*, 247-254.

Puigdefabregas, C., Samso, J., Serra-Kiel, J., & Tosquella, J. (1985). Facies Analysis and Faunal Assemblages of the Roda Sandstone Formation, Eocene of hte Southern Pyrenees. *IAS European Regional Meeting*, 639-642.

Russell, R. J. (1968). Where Most Grains of Very Coarse Sand and Fine Gravel are Deposited. *Sedimentology*, 31-38.

Russell, R. J. (1968). Where Most Grains of Very Coase Sand and Fine Gravel are Deposited. *Sedimentology*, 31-38.

Seybold, H., Andrade, J., & Herrmann, H. J. (2007). Modelling River Delta Formation. *PNAS*, 1-5.

Tinterri, R. (2007). The Lower Eocene Roda Sandstone (South-Central Pyrenees): an Example of a Flood Dominated River-Delta System in a Tectonically Controlled Basin. *Rivista Italiana di Paleontologia e Stratigrafia* , 223-255.

Trautmann, C. H., Kulhawy, F. H., & O'Rourke, T. D. (1985). Sand Density Measurements for Laboratory Studies. 159-165.

van der Vegt, H. (2018). *From Fluvial Supply to Delta Deposits, Simulating Sediment Delivery, Transport and Deposition.*

Wentworth, C. K. (1922). A Scale of Grade and Class Terms for Clastic Sediments. *The Journal of Geology*.

Willis, B. (2005). Deposits of Tide-Influenced River Deltas. *SEPM*.

Yang, C.-S., & Nio, S.-D. (1989). An ebb-tide delta depositional model - a comparison between the moern Eastern Scheldt tidal basin (southwest Netherlands) and the Lower Eocene Roda Sandstone in hte southern Pyrenees (Spain). *Sedimentology Geology*, 175-196.

8 Appendix

8.1 Appendix A - Basic Model Simulations

Before the field work took place, initial models were run. These models were basic in nature in that they were confined to one or two sediment input parameters. The goal of this test was to get an understanding of how the model runs and to gauge the computational time for the simulation. The grid and bathymetry were kept constant, with the sediment values being the only input parameters being altered.

Simulation 1

The first simulation that was run utilized a single sediment value as the input with a uniform grain size. In this case, very coarse sand is being deposited within the basin.

Sediment Classification	Sand
Specific density	2600 kg/m^3
Sediment Diameter	1 mm

Simulation 2

The second simulation is identical to simulation 1 in that only one sediment is acting as the input value. In this case, a carbonate sand is being deposited within the basin. This will show the affect that density has on the system.

Sediment Classification	Carbonate Sand
Specific density	2700 kg/m^3
Sediment Diameter	1 mm

The final of the initial simulations involved combining the two previously discussed sediments into one simulation. The properties of the sediments were not altered and a 50:50 ratio of sand to carbonate sand was used.

Sediment Classification	Density	Grain Size
Sand	2600 kg/m^3	1 mm
Carbonate Sand	2700 kg/m^3	1 mm

The models were run for 247 time steps. The results for each of the three models is shown below. The top left image represents the sand only simulation, the top right represents the carbonate sand only simulation, and the bottom image is the combination of the two sediments.

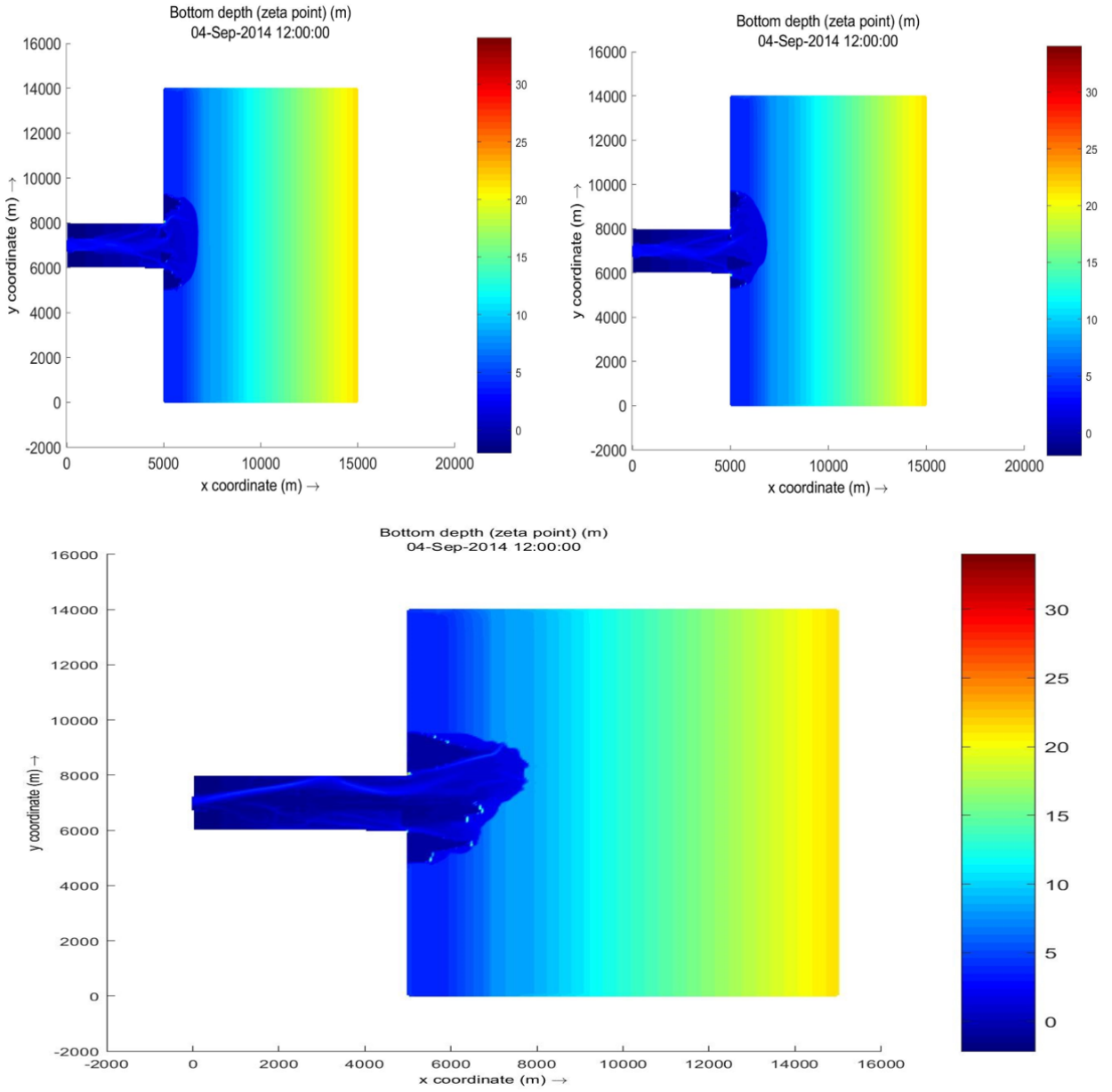

There are not any noticeable differences between the sand and carbonate sand only simulations. Both exhibit roughly the same shape and size, with the carbonate sand simulation displaying a slight migration to the left once it enters the basin. Due to the small amounts of sediment being deposited in these simulations, it is difficult to gather any noticeable affects that change in density has on the system. The simulation that combines the two sediments gives an early indication of how more complex models will look. The sand lobe progrades into the basin before moving laterally. These initial simulations were used as a way to understand the input parameters and ensure that modifications to the models will result in the simulations running correctly without errors.

8.2 Appendix B - Complex Simulations

Before the simulations involving the grain size analysis were run, an additional simulation was run that was more complex in nature than the first three simulations. The goal of this simulation was to utilize a total of six grain size classes to observe the resulting sand lobe shape. This also acted as a test to ensure simulations containing higher amounts of sediment input will run smoothly without errors. The same grid was kept constant but the bathymetry was altered. In the initial simulations, the river mouth had a width of two kilometers. For this simulation, the width of the river mouth is reduced to 950 meters to better represent the conditions during the time of deposition for the Roda. The river discharge is set to 1500 m^3/s and the waves are assigned a height of 0.5 meters. The sediment input values are shown in the table below.

Grain Size (mm) - Class	Concentration (kg/m^3)	Density (kg/m^3)
2000 - Very Coarse	0.0450	2600
1000 - Coarse	0.0150	2600
500 - Medium	0.0225	2600
200 - Fine	0.0300	2600
200 - Fine	0.0150	2700
70 - Very Fine	0.0225	2600
50 - Mud	0.0150	500

The results of the simulation are shown in the figure below.

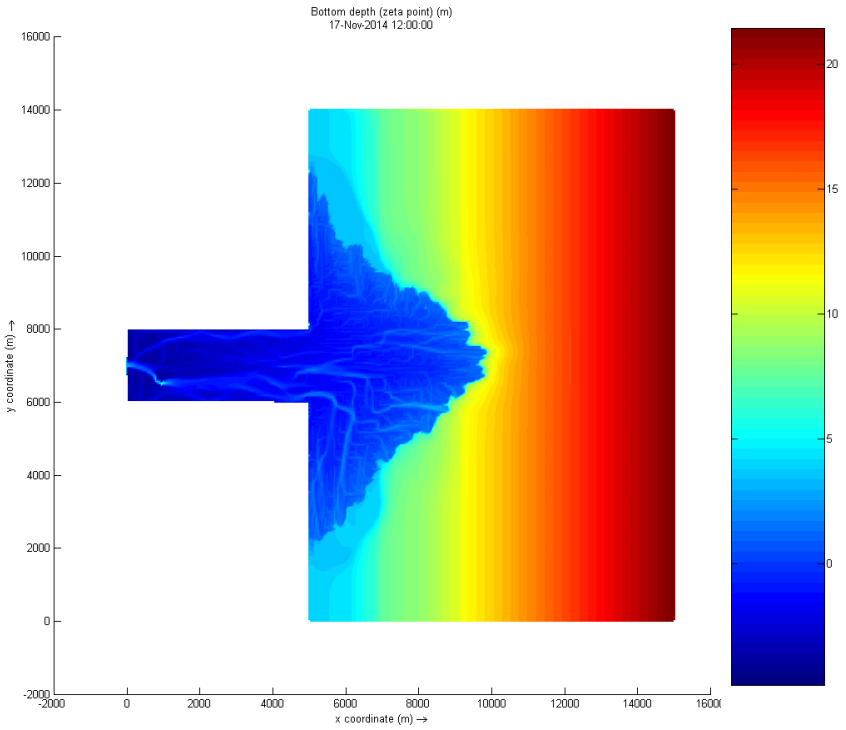

The resulting sand lobe contains a higher degree of complexity when compared to the previous simulations. The edge of the lobe reaches approximately five kilometers into the basin, and extends laterally four kilometers on each side. The arithmetic mean of the deposited sediment is shown below.

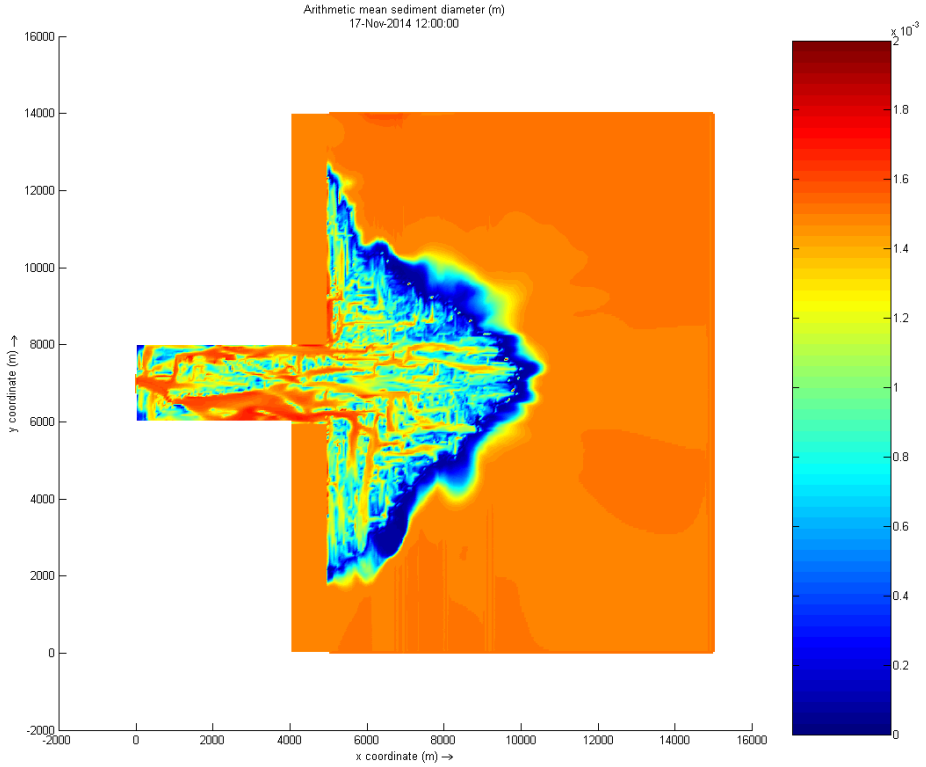

The image above shows the grain size distribution for the sand lobe. The finer grained sediments are found along the outer edges of the lobe, while the coarsest material is found within the channels in the more proximal settings. The majority of the lobe is made up of medium and fine grained sand that is deposited in locations where the channels are not found. This simulation provided insight on the depositional trends and the geometry of simulations containing larger amounts of sediment input values.

8.3 Appendix C - Images of Thin Sections

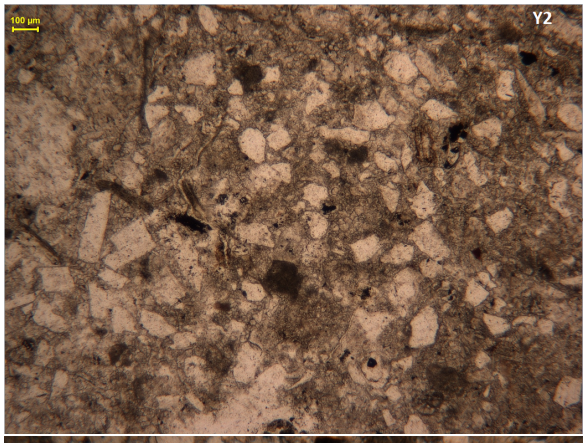

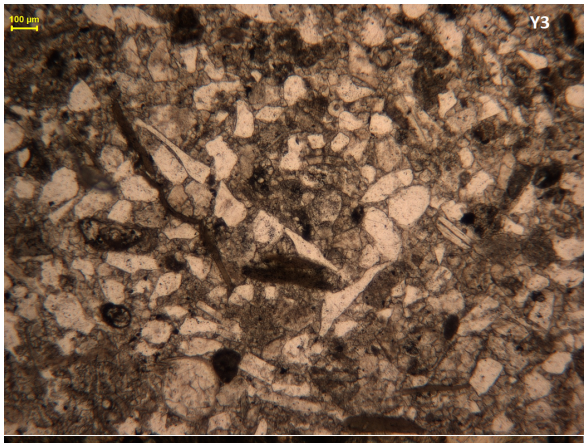

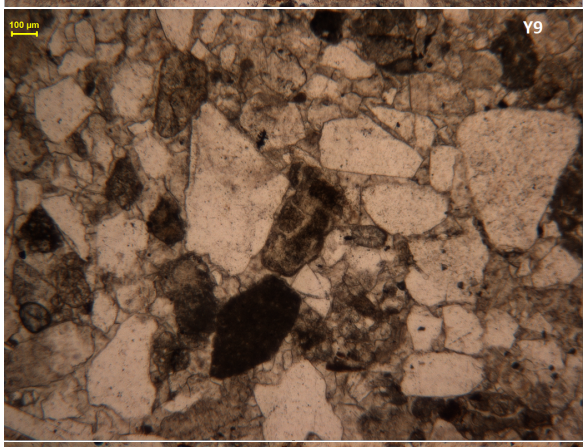

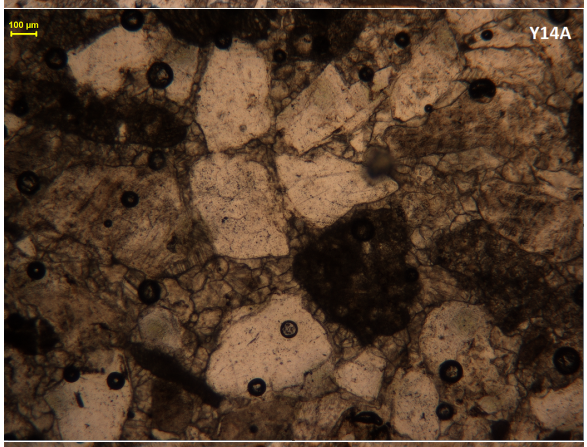

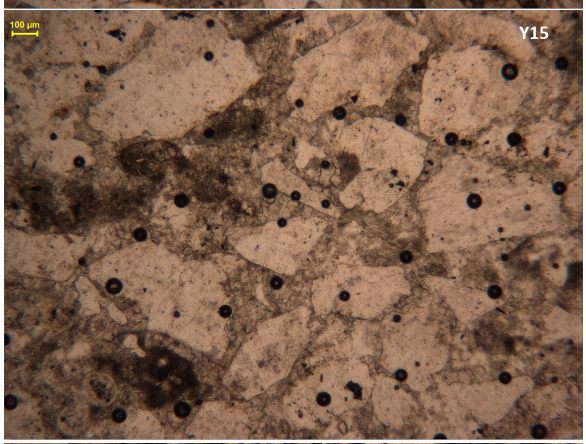

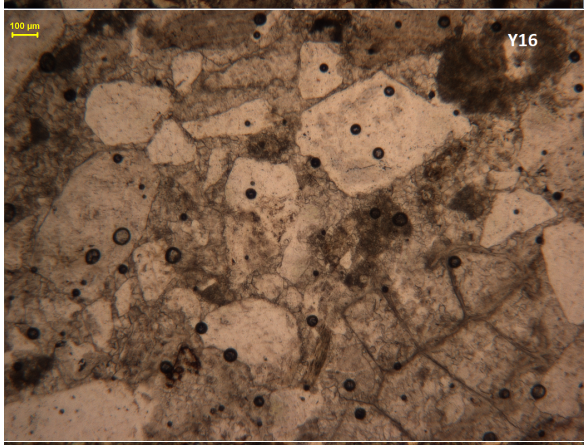

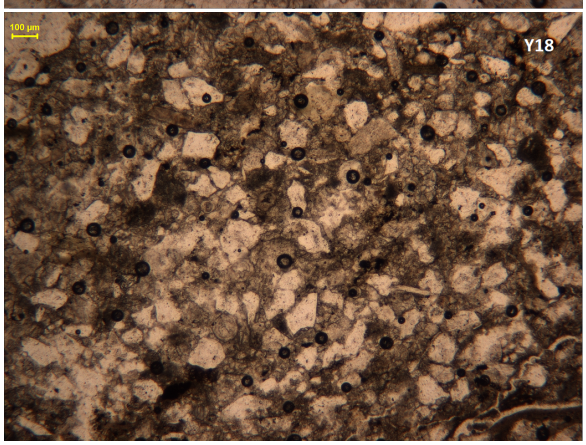

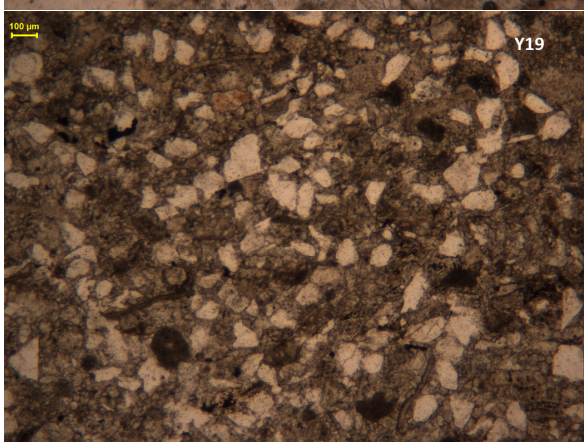

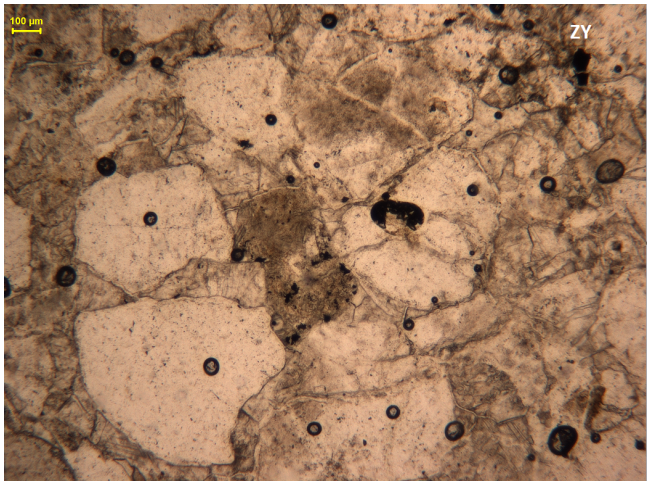
100 µm
ZY

8.4 Appendix D - MATLAB Code

The following MATLAB code was used to sort and prepare the data from the simulations. The resulting values represented the difference between the interpolation data and the simulation data.

```
%get grain size fraction per bookkeeping layer - 77 bookkeeping layers,
%last timeinterval
lyrfrac = ncread('O:\Models\thinfinalnomud\trim-coarse-sand.nc','LYRFRAC',[1 1 1
    1 321], [inf inf inf inf inf], [1 1 1 1 1]);
size(lyrfrac);
dp_bedlyr = ncread('O:\Models\thinfinalnomud\trim-coarse-sand.nc','DP_BEDLYR',[1
    1 1 321], [inf inf inf inf], [1 1 1 1]);
size(dp_bedlyr);
% first time interval
lyrfrac1 = ncread('O:\Models\thinfinalnomud\trim-coarse-sand.nc','LYRFRAC',[1 1
   1 1 1], [inf inf inf inf 1], [1 1 1 1 1]);
dp_bedlyr1 = ncread('O:\Models\thinfinalnomud\trim-coarse-sand.nc','DP_BEDLYR'
    ,[1 1 1 1], [inf inf inf 1], [1 1 1 1]);
X = ncread('O:\Models\thinfinalnomud\trim-coarse-sand.nc','XCOR');

%define layer thickness
lyrthick = zeros(size(lyrfrac,1),size(lyrfrac,2),size(lyrfrac,3));
lyrthick = dp_bedlyr(:,:,2:end) - dp_bedlyr(:,:,1:end-1);
lyrthick1 = zeros(size(lyrfrac1,1),size(lyrfrac1,2),size(lyrfrac1,3));
lyrthick1 = dp_bedlyr1(:,:,2:end) - dp_bedlyr1(:,:,1:end-1);

% example of data at location 180, 150
well1_thickness  = squeeze(squeeze(lyrthick(180,150,:)));
well1_sedfrac = squeeze(squeeze(lyrfrac(180,150,:,:)));

%total thickness of each GS class
lyrthick_expand = repmat(lyrthick,[1,1,1,6]);
lyrthick_expand1 = repmat(lyrthick1,[1,1,1,6]);

sed_end = lyrfrac.*lyrthick_expand;
sed_start = lyrfrac1.*lyrthick_expand1;

%summed thickness
temp = cumsum(sed_end,3);
sed_end_summed = squeeze(temp(:,:,end,:));
```

```
temp = cumsum(sed_start,3);
sed_end_start = squeeze(temp(:,:,end,:));


sed_deposited_vol = sed_end_summed - sed_end_start;
%remove sed classess that are eroded
sed_deposited_vol(sed_deposited_vol < 0) = 0;
%use volume fractions
temp = cumsum(sed_deposited_vol,3);
temp = squeeze(temp(:,:,end));
temp = repmat(temp,[1,1,6]);
sed_deposited_volfrac = sed_deposited_vol ./ temp;

%use mass fractions
temp = [1600, 1600, 1600, 1600, 1600, 500]';
temp = repmat(temp,[1,282,302]);
temp = permute(temp,[2,3,1]);
sed_deposited_mass = sed_deposited_vol.* temp;


temp = cumsum(sed_deposited_mass,3);
temp = squeeze(temp(:,:,end));
temp = repmat(temp,[1,1,6]);
sed_deposited_massfrac = sed_deposited_mass ./ temp;
temp = sed_deposited_massfrac(:,:,6);
temp(temp > 0.9) = 0;
sed_deposited_massfrac(:,:,6) = temp;

 values_set1 = sed_deposited_massfrac(:,:,1);
 values_set2 = sed_deposited_massfrac(:,:,2);
 values_set3 = sed_deposited_massfrac(:,:,3);
 values_set4 = sed_deposited_massfrac(:,:,4);
 values_set5 = sed_deposited_massfrac(:,:,5);

%     X_values(:,i) = a(:,
%% read in mas fraction values for interpoalted field data and calculated
    difference

% create field_interp_set1
```

```
70 temp = dlmread('O:\Grain Size\finefinal.xyz',' ');
71 field_interp_set1 = [(squeeze(temp(:,4))-1)/50 (squeeze(temp(:,7))-1)/50 squeeze
       (temp(:,10))];
72
73 model_set1 = field_interp_set1;
74 % values_set1 = sed_deposited_volfrac(83:175,123:220,1);
75 for i = 1:size(field_interp_set1,1)
76     model_set1(i,3) = sed_deposited_massfrac(floor(field_interp_set1(i,2)),floor
           (field_interp_set1(i,1)),3);
77 end
78
79 diff_massfrac = field_interp_set1;
80 diff_massfrac(:,3) = field_interp_set1(:,3) - model_set1(:,3);
```